ISSN 1023-9855

胸腔醫學

Thoracic Medicine

The Official Journal of Taiwan Society of Pulmonary and Critical Care Medicine

Vol.25 No.5 Oct. 2010

第二十五卷 第五期

中華民國九十九年十月

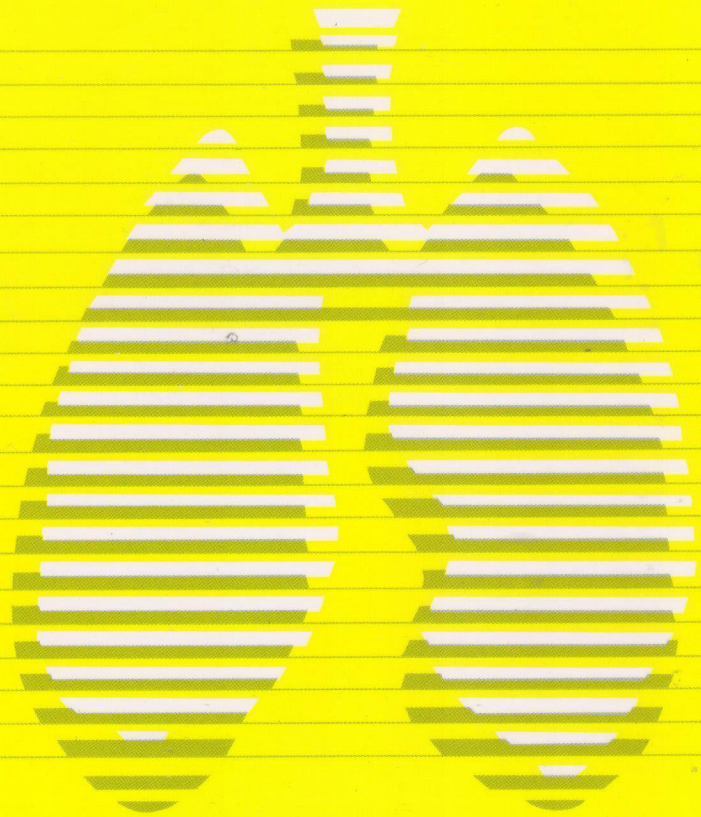

台灣胸腔暨重症加護醫學會

桃園縣龜山鄉復興街五號

5. Fu-Hsing Street, Kuei Shan Hsiang,
Taoyuan Hsien, Taiwan, R.O.C.

ISSN 1023-9855

中華民國九十九年十月　第二十五卷　第五期

ISSN 1023－9855

胸腔醫學

Thoracic Medicine

The Official Journal of Taiwan Society of Pulmonary and Critical Care Medicine

Vol.25 No.5 October 2010

原著

病例報告

中華民國九十九年十月　第二十五卷　第五期

ISSN 1023－9855

Vol.25 No.5 October 2010

胸腔醫學

Thoracic Medicine

The Official Journal of Taiwan Society of Pulmonary and Critical Care Medicine

Orginial Articles

Case Reports

RIFLE Classification Did Not Have Satisfactory Predictive Value for Septic Patients with High Severity Scores

Chih-Yu Huang, Heng-Jung Hsu*, Yu-Chih Liu, Chung-Ching Hua, Huang-Ping Wu

Background: Predicting the outcome of patients with severe sepsis is important. The RIFLE classification has been evaluated for its ability to predict mortality. The aim of this study was to compare the predictive value of 3 scoring systems: the Acute Physiology and Chronic Health Evaluation (APACHE) II score, the Multiple Organ Dysfunction Score (MODS), and the Risk, Injury, Failure, Loss of kidney function, and End-stage kidney disease (RIFLE) classification.

Patients and methods: Seventy-one severe septic patients admitted to intensive care units (ICU) directly from the emergency department were enrolled into this study. The APACHE II score, MODS, and RIFLE classification were calculated within 24 hours after admission. Areas under the receiver operating characteristic (ROC) curves were computed in order to analyze the discriminatory power of these 3 scoring systems.

Results: The value of the APACHE II score and the MODS in the non-survivors was statistically significantly higher than that in the survivors. The RIFLE classification showed no significant difference between survivors and non-survivors. Areas under the ROC curves were 0.801, 0.715, and 0.602, respectively, for the APACHE II score, the MODS, and the RIFLE classification. The APACHE II score and the MODS were better tools for outcome prediction, compared with the RIFLE classification. The discriminatory power of the RIFLE classification did not have significance (p = 0.226) for outcome prediction in severe septic patients.

Conclusions: The APACHE II score and the MODS were useful tools in patients with severe sepsis. The RIFLE classification did not show satisfactory power in predicting 28-day mortality in more severe septic patients. ***(Thorac Med 2010; 25: 230-237)***

Key words: severe sepsis, mortality, RIFLE, APACHE II, MODS

Introduction

Severe sepsis is not only a common health-care problem but also a frequently fatal condition, and is still a predominant problem in intensive care units (ICUs) [1-2]. Sepsis may have a

Division of Pulmonary, Critical Care, and Sleep Medicine, Chang Gung Memorial Hospital at Keelung, Chang Gung University, Taoyuan; Department of Respiratory Therapy, Chang Gung Memorial Hospital at Keelung; *Department of Nephrology, Chang Gung Memorial Hospital at Keelung, Chang Gung University, Taoyuan
Address reprint requests to: Dr. Huang-Ping Wu, Division of Pulmonary, Critical Care, and Sleep Medicine, Chang Gung Memorial Hospital at Keelung, No 222, Maijin Rd., Anle District, Keelung City, 204, Taiwan

progressive course and result in multiple-organ dysfunction, which is the leading cause of mortality in ICU patients. We need tools such as the Acute Physiology and Chronic Health Evaluation (APACHE) II score and the Multiple Organ Dysfunction Score (MODS) to evaluate the severity of illness and risk of mortality for these patients [3-4]. Prognostic tools should have the following features: ease of use and clinical applicability, and high sensitivity and specificity for a variety of populations [5].

Acute kidney injury (AKI) is an important issue, and increases mortality among patients with severe sepsis [6]. The Acute Dialysis Quality Initiative (ADQI) proposed a consensus definition for the Risk, Injury, Failure, Loss of kidney function, and End-stage kidney disease (RIFLE) classification for acute kidney injury, grading the severity into risk, injury, and failure. Recently, several studies have used the RIFLE for outcome prediction in ICU patients, and its practicability is still under discussion [7-11].

The purpose of this study was to compare the efficacy of these 3 scoring systems (APACHE II score, MODS, and RIFLE criteria) for outcome prediction in patients with severe sepsis.

Materials and Methods

Patients

Patient data from our previous prospective study [12] were used for analysis. The RIFLE classification was added retrospectively. From October 2003 to September 2005, 71 patients who were admitted to the emergency department and soon transferred to the ICU at Chang Gung Memorial Hospital due to severe sepsis were enrolled into this study. Exclusion criteria included a history of renal replacement therapy for end-stage renal disease. The ICU is a closed-format unit covered by medical intensivists. The following patient data were recorded within the first 3 days after admission: age, gender, medical history, infection source, and co-morbidity. Standard treatment, including fluid resuscitation, broad-spectrum antibiotics, drainage, and basic support, were provided to all patients. Antibiotics and fluid resuscitation were started as soon as possible after the sepsis was diagnosed [13]. Pneumonia was diagnosed based on new abnormal infiltration shown on the chest radiograph with fever or respiratory symptoms. Urinary tract infection was diagnosed based on the presence of pyuria and positive bacteria culture.

Severe sepsis and septic shock were defined according to the criteria of the Consensus Conference [14]. Systemic inflammatory response syndrome (SIRS) was defined as 2 or more of the following criteria: (1) body temperature $> 38^{o}C$ or $< 36^{o}C$; (2) respiratory rate > 24 breaths/min; (3) heart rate > 90 beats/min; and (4) white blood count > 12,000/μl or < 4,000/μl or > 10% bands. Sepsis was defined as SIRS according to a confirmed or suspected microbial etiology. Severe sepsis was defined as sepsis with 1 or more of organ dysfunction or hypotension. Septic shock was defined as sepsis with hypotension unresponsive to fluid resuscitation, which further required vasopressors to maintain blood pressure on the emergency department admission day. The survivors were defined as patients who were still alive 28 days after hospital admission. Disease severity was assessed by the APACHE II score, MODS, and RIFLE classification using the data within 24 hours of admission. Both the serum creatinine and urine output criteria were used to determine the

RIFLE classification of all patients. The criteria that led to the worst possible classification was used. Because some patients (n = 25, 35%) did not have baseline renal function, a hypothetical baseline serum creatinine was estimated for a given patient, assuming a normal glomerular filtration rate (75 ml/min per 1.73 m^2) with the modification of diet in renal disease (MDRD) formula, as recommended by the ADQI workgroup [15-16]. Patients were classified into 1 of the first 3 levels: risk (1 point), injury (2 points), and failure (3 points) according to the RIFLE classification. The non-AKI group was classified as 0 points [9].

Statistical analysis

Differences in age, APACHE II score, MODS, and RIFLE categories between the survivors and non-survivors were analyzed by T-test. Differences for categorical variables of gender, medical history, infection source, and co-morbidity between survivors and non-survivors were compared using the Chi-square test. Areas under the receiver operating characteristic (ROC) curves were calculated in order to analyze the discriminatory power of the scoring systems for outcome prediction. All statistical tests were 2-tailed and a *p* value less than 0.05 was considered statistically significant.

Results

Seventy-one patients were enrolled into this study and 15 patients (21.1%) died. The clinical characteristics and demographic data of the patients are shown in Table 1. The value of the APACHE II score and the MODS in the non-survivors was statistically significantly higher than that in the survivors. The RIFLE classification did not show a significant difference between the survivors and non-survivors. There were no significant differences in history and infection source between the survivors and non-survivors. The proportions of septic shock and gastrointestinal bleeding in the non-survivors were significant higher than in the survivors.

The ROC curves of the APACHE II score, the MODS, and the RIFLE classification are shown in Figure 1. Table 2 compares the discriminatory power of the 3 scoring systems. The areas under the ROC curves of the APACHE II score and the MODS were significantly different than 0.5, and that of RIFLE classification was not.

Discussion

In recent years, several scoring systems, such as the APACHE II and the MODS, have been used extensively to describe the severity of illness and predict the outcome of ICU patients. Besides, these systems can also be used to assist in clinical trials and to compare the quality of care in different ICUs [3-4]. Nevertheless, we still need a simple, fast, and accurate tool to predict the prognosis of ICU sepsis patients.

In 2004, the ADQI workgroup published a classification system for acute kidney injury. The system was given the acronym RIFLE (Risk, Injury, Failure, Loss of kidney function, and End-stage kidney disease). Recently, the RIFLE classifications ‘‘risk,’’ ‘‘injury,’’ and ‘‘failure’’ have been used to evaluate and predict the outcome of critically ill patients [16-17]. Several large retrospective and prospective studies have shown that the RIFLE classification was an independent risk factor for the hospital mortality of ICU patients [8, 10-11]. The studies of Lopes *et al*. and Chen *et al*. showed that the RIFLE classification is predictive of

Table 1. Clinical characteristics of severe sepsis patients (mean ± standard error mean, number and percentage).

Characteristic	Survivors (n = 56)	Non-survivors (n = 15)
Age (years)	70.2 ± 1.9	72.1 ± 3.3
Gender		
Male	32 (57.1)	7 (46.7)
Female	24 (42.9)	8 (53.3)
APACHE II score	22.3 ± 0.9	30.1 ± 2.0*
MODS	6.1 ± 0.3	7.9 ± 0.6*
RIFLE	0.8 ± 0.1	1.3 ± 0.3
History		
Chronic lung disease	17 (30.4)	5 (33.3)
Chronic renal disease	7 (12.5)	2 (13.3)
Liver cirrhosis	1 (1.8)	0 (0)
Diabetes mellitus	15 (26.8)	6 (40.0)
Heart failure	5 (8.9)	2 (13.3)
Old cerebrovascular accident	35 (62.5)	7 (46.7)
Hypertension	28 (50.0)	7 (46.7)
Source of sepsis		
Pneumonia	48 (85.7)	11 (73.3)
Urinary tract infection	6 (10.7)	3 (20.0)
Others	2 (3.6)	1 (6.7)
Co-morbidity		
Septic shock	19 (33.9)	11 (73.3)*
Bacteremia	10 (17.9)	4 (26.7)
Jaundice	10 (17.9)	3 (20.0)
Thrombocytopenia	23 (41.1)	8 (53.3)
Gastrointestinal bleeding	14 (25.0)	10 (66.7)*

* Statistical significance based on Chi-square test or Fisher's exact test for categorical variables, T-test for continuous variables.

Abbreviations: APACHE = Acute Physiology and Chronic Health Evaluation; MODS = Multiple Organ Dysfunction Score; RIFLE = Risk, Injury, Failure, Loss of kidney function, and End-stage kidney disease

Table 2. The areas under the ROC (mean ± standard error mean) analysis of the 3 scoring systems.

	Areas under ROC	95% CI	*p* value
APACHE II	0.801 ± 0.064	0.675 – 0.926	< 0.001
MODS	0.715 ± 0.068	0.582 – 0.848	0.011
RIFLE	0.602 ± 0.087	0.432 – 0.773	0.226

Abbreviations: ROC = receiver operating characteristic; CI = confidence interval; APACHE = Acute Physiology and Chronic Health Evaluation; MODS = Multiple Organ Dysfunction Score; RIFLE = Risk, Injury, Failure, Loss of kidney function, and End-stage kidney disease

mortality in patients with severe sepsis [7, 9].

In our study, all patients were recruited from the emergency department and the mean of the APACHE II score was 23.9 (survivors: 22.3, non-survivors: 30.1). We found that the APACHE II score and the MODS were still

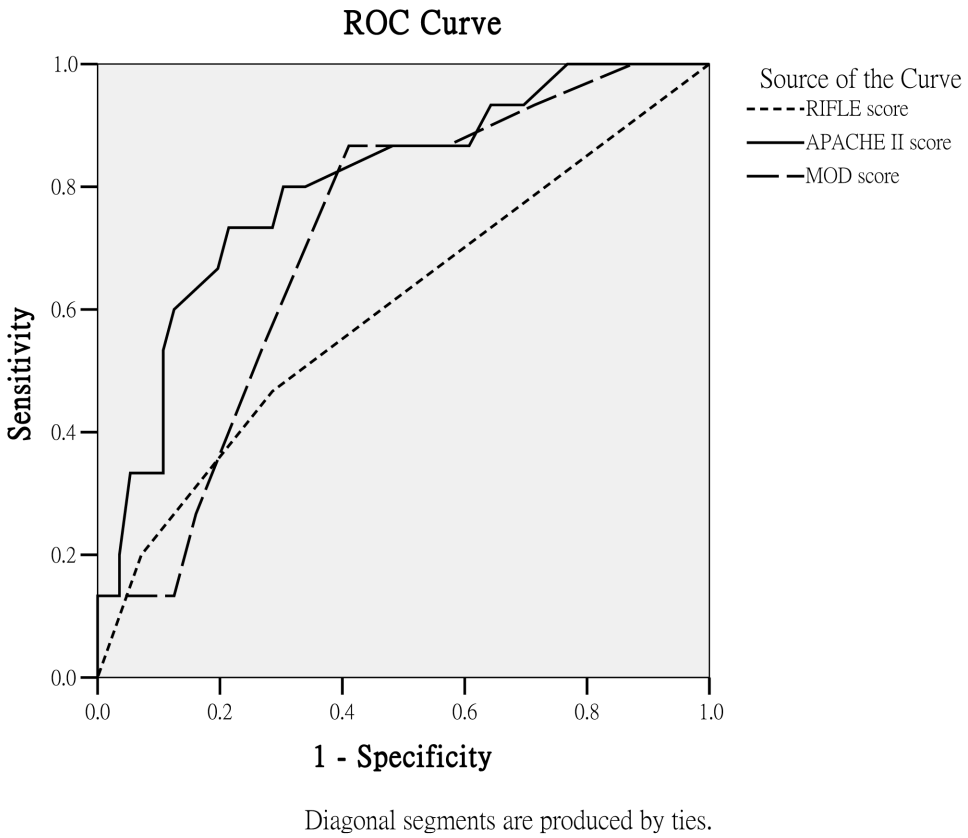

Fig. 1. ROC (receiver operating characteristic) curves of the APACHE (Acute Physiology and Chronic Health Evaluation) II score, MODS (Multiple Organ Dysfunction Score), and RIFLE (Risk, Injury, Failure, Loss of kidney function, and End-stage kidney disease) classification.

useful prognostic tools in this group. Nevertheless, the RIFLE classification did not have good discriminative power for hospital mortality in more severe sepsis patients (mean APACHE II score: 23.9). Ahlstrom *et al*. also found that the RIFLE score did not have good discriminative power (AUROC: 0.653) regarding hospital outcome in critically ill patients [8]. Contrary to our results, Ostermann *et al*. performed a retrospective analysis of a database of 41,972 patients admitted to 22 ICUs. He concluded that the RIFLE classification was proper for defining AKI in the ICU, and was associated with hospital outcome. However, the level of severity of the patients in the study was relatively low (median APACHE II score of the survivors: 12, non-survivors: 21) [11]. Similarly, Chen *et al*. reported that the RIFLE classification could predict prognosis in ICU sepsis patients. The survivors and non-survivors had mean APACHE II scores of 18 and 23, respectively [9].

The patient populations were different in the above studies. The patient population we enrolled had been admitted to the ICU directly from the emergency department. The Ostermann *et al*. and Chen *et al*. studies enrolled patients from both the emergency department and medical wards [9, 11], which might have led to different results. According to the APACHE

scoring system, the severity of disease in our patients was greater. It seems that the RIFLE classification did not have satisfactory predictive power for hospital mortality in patients with severe sepsis with a high APACHE II score. The RIFLE classification may be able to predict exactly the outcome of patients with a relatively low APACHE II score, but not the outcome of patients with a high APACHE II score.

There are some limitations to this study. First, some patients did not have available baseline creatinine to calculate the proportional decrease of renal function. Thus, we used an estimated baseline creatinine, based on the MDRD equation proposed by the ADQI in previous studies [8-10]. Second, Cruz *et al*. found that serum creatinine criteria appeared to be a better predictor than urine output criteria. Increased serum creatinine is an earlier sign of deterioration of renal function than oliguria [10]. These limitations may have influenced the results to a certain degree.

In conclusion, the APACHE II scores and the MODS differed between the survivors and non-survivors with severe sepsis. Nevertheless, the RIFLE classification did not provide satisfactory power to predict mortality in patients with severe sepsis with a high APACHE II score.

References

1. Linde-Zwirble WT, Angus DC. Severe sepsis epidemiology: sampling, selection, and society. Crit Care 2004; 8: 222-6.
2. Angus DC, Linde-Zwirble WT, Lidicker J, *et al*. Epidemiology of severe sepsis in the United States: analysis of incidence, outcome, and associated costs of care. Crit Care Med 2001; 29: 1303-10.
3. Marshall JC, Cook DJ, Christou NV, *et al*. Multiple organ dysfunction score: a reliable descriptor of a complex clinical outcome. Crit Care Med 1995; 23: 1638-52.
4. Knaus WA, Draper EA, Wagner DP, *et al*. APACHE II: a severity of disease classification system. Crit Care Med 1985; 13: 818-29.
5. Vincent JL, Ferreira F, Moreno R. Scoring systems for assessing organ dysfunction and survival. Crit Care Clin 2000; 16: 353-66.
6. Brun-Buisson C, Meshaka P, Pinton P, *et al*. EPISEPSIS: a reappraisal of the epidemiology and outcome of severe sepsis in French intensive care units. Intensive Care Med 2004; 30: 580-8.
7. Lopes JA, Jorge S, Resina C, *et al*. Prognostic utility of RIFLE for acute renal failure in patients with sepsis. Crit Care 2007; 11: 408.
8. Ahlstrom A, Kuitunen A, Peltonen S, *et al*. Comparison of 2 acute renal failure severity scores to general scoring systems in the critically ill. Am J Kidney Dis 2006; 48: 262-8.
9. Chen YC, Jenq CC, Tian YC, *et al*. RIFLE classification for predicting in-hospital mortality in critically ill sepsis patients. Shock 2009; 31: 139-45.
10. Cruz DN, Bolgan I, Perazella MA, *et al*. North East Italian Prospective Hospital Renal Outcome Survey on Acute Kidney Injury (NEiPHROS-AKI): targeting the problem with the RIFLE Criteria. Clin J Am Soc Nephrol 2007; 2: 418-25.
11. Ostermann M, Chang RW. Acute kidney injury in the intensive care unit according to RIFLE. Crit Care Med 2007; 35: 1837-43.
12. Wu HP, Chen CK, Chung K, *et al*. Serial cytokine levels in patients with severe sepsis. Inflamm Res 2009; 58: 385-93.
13. Rivers E, Nguyen B, Havstad S, *et al*. Early goal-directed therapy in the treatment of severe sepsis and septic shock. N Engl J Med 2001; 345: 1368-77.
14. Levy MM, Fink MP, Marshall JC, *et al*. 2001 SCCM/ESICM/ACCP/ATS/SIS International Sepsis Definitions Conference. Crit Care Med 2003; 31: 1250-6.
15. National Kidney Foundation. K/DOQI clinical practice guidelines for chronic kidney disease: evaluation, classification, and stratification. Am J Kidney Dis 2002; 39: S1-266.
16. Bellomo R, Ronco C, Kellum JA, *et al*. Acute renal failure - definition, outcome measures, animal models, fluid therapy and information technology needs: the

Second International Consensus Conference of the Acute Dialysis Quality Initiative (ADQI) Group. Crit Care 2004; 8: R204-12.

17. Ricci Z, Cruz D, Ronco C. The RIFLE criteria and mortality in acute kidney injury: A systematic review. Kidney Int 2008; 73: 538-46.

在高嚴重程度分數的嚴重敗血症病人身上使用 RIFLE classification 沒有令人滿意的預測價值

黃志宇　許恆榮*　劉育志　花仲涇　吳黃平

前言：預測嚴重敗血症病人的結果是重要的。RIFLE classification已經被拿來評估預測病人死亡的能力。本研究的目標是使用3個評分系統包括APACHE (Acute Physiology and Chronic Health Evaluation) II score、MODS (Multiple Organ Dysfunction Score)、及RIFLE (Risk, Injury, Failure, Loss of kidney function, and End-stage kidney disease) classification來比較其預測結果的價值。

方法：這個研究收集了71個從急診部門直接住到加護病房的嚴重敗血症病人。他們的APACHE II score、MODS、及RIFLE classification在住院後的24小時內就計算好。我們也估算了ROC (receiver operating characteristic) 的曲線下面積來分析這3個評分系統的辨識能力。

結果：非存活者的APACHE II score及MODS的數值皆顯著高於存活者的平均分數，但RIFLE classification在非存活者及存活者之間並沒有統計上的差異。APACHE II score、MODS、及RIFLE classification的ROC曲線下面積分別是0.801、0.715及、0.602。APACHE II score及MODS比起RIFLE classification而言，是用來預測結果比較好的工具。RIFLE classification的辨識能力在預測嚴重敗血症病人的結果上並沒有顯著意義 ($p = 0.226$)。

結論：APACHE II score及MODS對於嚴重敗血症病人而言是有用的工具。而RIFLE classification使用在相對嚴重的敗血症病人來預測28天的死亡率並沒有令人滿意的預測能力。*(胸腔醫學 **2010; 25: 230-237**)*

關鍵詞：嚴重敗血症，死亡率，RIFLE，APACHE II，MODS

長庚大學　基隆長庚紀念醫院　胸腔、重症、暨睡眠科，基隆長庚紀念醫院　呼吸治療科
*長庚大學　基隆長庚紀念醫院　腎臟內科
索取抽印本請聯絡：吳黃平醫師，基隆長庚紀念醫院　胸腔、重症、暨睡眠科，基隆市麥金路222號

Coexisting Invasive Pulmonary Aspergillosis and Active Tuberculosis in a Patient with End-stage Renal Disease

Da-Wei Wu*, Chih-Jen Yang*,**, Ying-Ming Tsai*, Jhi-Jhu Huang*,***, Ming-Shyan Huang*,**, Tung-Heng Wang*,***

Invasive pulmonary aspergillosis is 1 of the most aggressive fungal infections, often occurring in patients with a severely immunocompromised status. Taiwan has a high prevalence rate of end-stage renal disease (ESRD), and is an endemic area for tuberculosis (TB). Coexisting TB and invasive pulmonary aspergillosis, however, has not been reported in Taiwan.

A 77-year-old female with ESRD had received regular hemodialysis for 1 and a half years. She presented with a high fever, cough, and pain in her left forearm at the arteriovenous shunt site for 3 days. The initial chest radiograph revealed opacity in the entire left lung. Thoracocentesis obtained exudative pleural effusion. Sputum acid-fast stain was positive, and anti-tuberculous therapy was started. Sputum culture also grew *Mycobacterium tuberculosis* later. Fever persisted despite anti-tuberculous therapy.

Subsequent chest radiograph and computed tomography (CT) showed multiple opacities. CT-guided lung biopsy showed hyphae and conidia. Lung biopsy culture revealed *Aspergillus fumigatus*. Despite anti-fungal therapy, the patient died of septic shock and multiple-organ failure. We discussed the predisposing factors, diagnosis and treatment of invasive pulmonary aspergillosis, and the possibility of coexistent TB and invasive aspergillosis in patients with ESRD in Taiwan. ***(Thorac Med 2010; 25: 238-244)***

Key words: invasive aspergillosis, pulmonary tuberculosis, end-stage renal disease

Introduction

Aspergillus-related infection is an important fungal infection, and the clinical presentations include invasive pulmonary aspergillosis, chronic necrotizing pulmonary aspergillosis, allergic bronchopulmonary aspergillosis and aspergilloma. Invasive pulmonary aspergillosis is 1 of the most aggressive fungal infections, often occurring in patients with a severely im-

* Division of Pulmonary and Critical Care Medicine, Department of Internal Medicine, Kaohsiung Medical University Hospital; ** Department of Internal Medicine, Faculty of Medicine, College of Medicine, Kaohsiung Medical University, Taiwan; *** Faculty of Respiratory Care, College of Medicine, Kaohsiung Medical University, Taiwan

Address reprint requests to: Dr. Tung-Heng Wang, Division of Pulmonary and Critical Care Medicine, Department of Internal Medicine, Kaohsiung Medical University Hospital, # 100, Tzyou 1st Road, Kaohsiung 807, Taiwan

munocompromised status, such as those with prolonged and severe neutropenia, those under glucocorticoid therapy, those having had hematopoietic stem cell and solid organ transplantation, and those with advanced AIDS [1-2]. Taiwan has the highest incidence and highest prevalence rate of end-stage renal disease (ESRD) in the world [3]. Patients with ESRD are prone to having fungus infection [4].

Taiwan is also an endemic area for tuberculosis (TB) infection, with an incidence rate of 62.0 per 100,000 patients and a mortality rate of 3.3 per 100,000 patients in 2008 [5]. The incidence of TB among patients with ESRD is 10 to 25-fold higher than in the general population [6]. Thus, the occurrence of coexistent active pulmonary TB and invasive aspergillosis in ESRD patients is possible, though it has never been documented in Taiwan. Herein, we report a patient with ESRD, fever, arteriovenous (AV) shunt infection and pneumonia. Sputum culture grew *Mycobacteria tuberculosis*. Lung biopsy histology revealed hyphae and conidia, and biopsy specimens grew *Aspergillus fumigatus*.

Case Report

A 77-year-old female with hypertension, congestive heart failure, peptic ulcer and reflux esophagitis was diagnosed with ESRD, and had undergone regular hemodialysis for 1 and a half years. She was brought to the emergency department of Kaohsiung Medical University Hospital due to high fever, cough and local pain in her left forearm at the AV shunt site for 3 days. Upon arriving at our emergency room, her consciousness was drowsy and body temperature was 37.9^{o}C. She had decreased breathing sounds in the left side of the chest, and local tenderness and swelling in the AV shunt area of her left forearm. Chest radiograph (Figure 1A) revealed total opacification of the left hemitho-

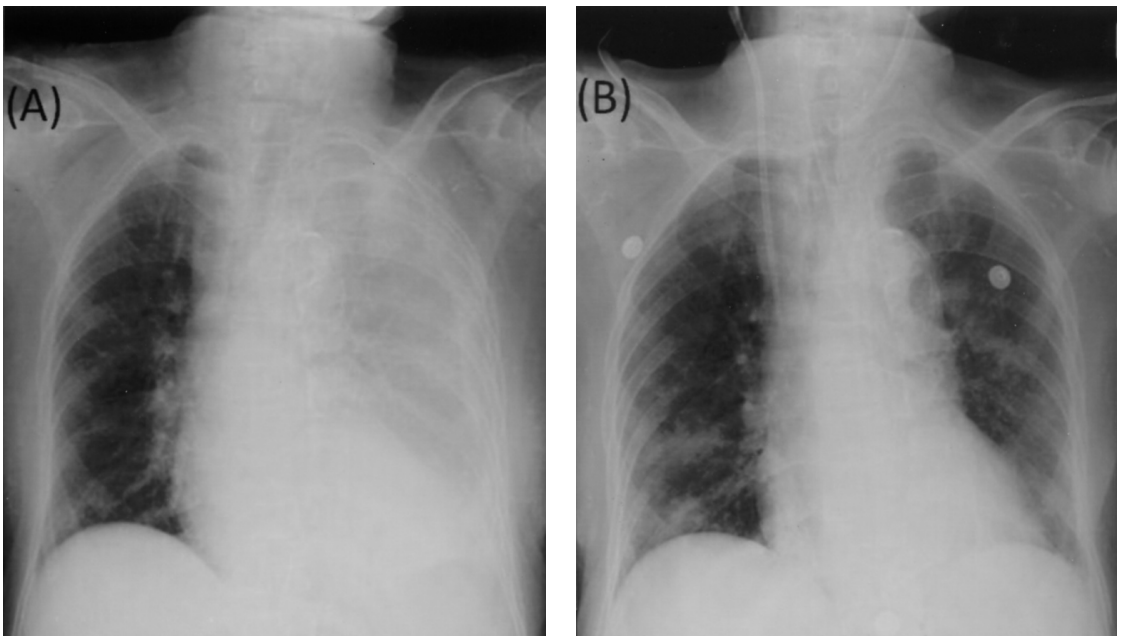

Fig. 1. Chest radiograph at admission shows opacity in the entire left lung (1A). Chest radiograph taken on the 23th admission day shows disappearance of the left pleural effusion, but the existence of several patchy opacities in both lungs (1B).

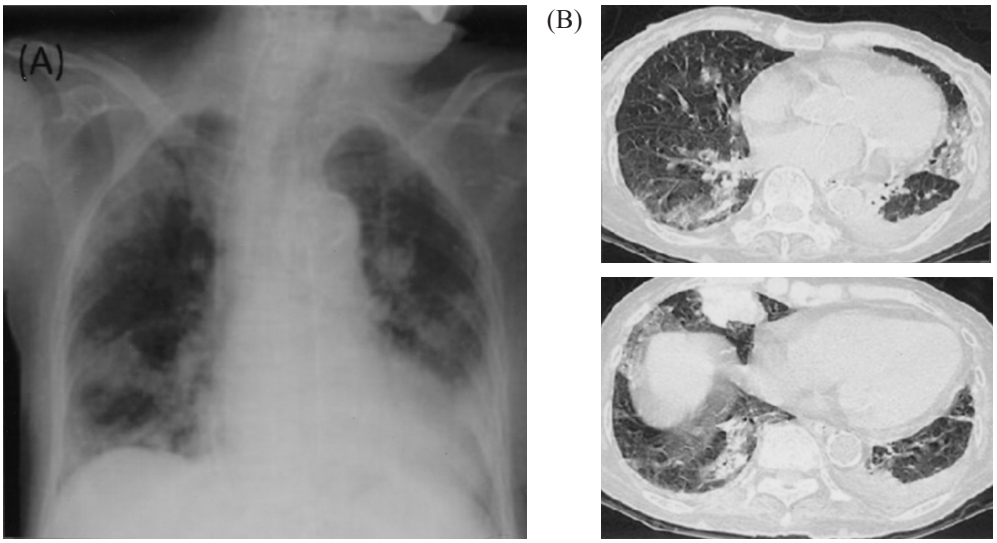

Fig. 2. Chest radiograph (2A) taken on the 74th admission day and CT (2B) on the 78th admission day showed several new nodules and wedge-shaped consolidations in both lungs, along with ground glass opacities and bilateral pleural effusions.

rax. Thoracocentesis obtained exudative pleural effusion with lymphocyte predominance. She was admitted and received cefmetazole 2 g per day for pneumonia and shunt infection. However, fever persisted even though her AV shunt infection gradually improved. Blood culture sampled at the emergency service grew *Staphylococcus epidermidis*. Pleural fluid culture yielded no bacteria, fungi or mycobacteria. Subsequent chest radiograph (Figure 1B) showed patchy shadows in both lungs, and sputum acid-fast stain was positive. We then started anti-TB therapy with rifampin 600 mg, isoniazid 300 mg, and pyrazinamide 1000 mg per day, and ethambutol 800 mg every 2 days on the 28th admission day. Later, her sputum culture grew *Mycobacterium tuberculosis* and the strain was resistant to isoniazid. We then discontinued isoniazid and continued the other anti-tuberculous agents.

However, low-grade fever persisted despite anti-TB treatment for several weeks. A subsequent chest radiograph showed that previous mass shadows were enlarged and had become confluent (Figure 2A). Chest computed tomography (CT) revealed that the mass shadows were wedge-shaped consolidations at the right middle, right lower and left lingular lobe. There were also ground glass opacities and small nodules in both lungs, as well as bilateral pleural effusions (Figure 2B). Fungal pneumonia was suspected because of her poor clinical response to broad-spectrum antibiotics. Oral voriconazole 400 mg per day was prescribed on the 78th admission day. We also performed CT-guided biopsy from a mass in the right lower lobe.

Histologic examination using hematoxylin and eosin (H&E) stain showed calcified, degenerated, septated fungal hyphae and conidial heads associated with granulomatous inflammation and fibroblastic proliferation. The findings were characteristic of *Aspergillus* infection. Finally, lung specimens grew *Aspergillus fumigatus*, which was also demonstrated using lactophenol cotton blue stain (Figure 3). Therefore, we started amphotericin B 45 mg per day after

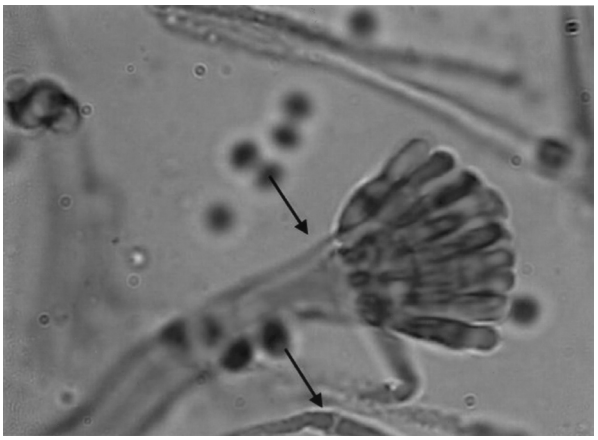

Fig. 3. The septated hyphae structure and conidial head suggested *Aspergillus* infection (lactophenol cotton blue stain, 1000X).

a 5-day voriconazole treatment course.

We also checked serum *Aspergillus galactomannan* (Platelia®, Aspergillus enzyme-linked immunosorbent assay, Bio-Rad Laboratories), but it was negative. Unfortunately, the persistent high fever and high C-reactive protein indicated treatment failure. We shifted amphotericin B to caspofungin 50 mg per day after an 11-day treatment course. We also started trimethoprim-sulfamethoxazole to cover *Pneumocystis jirovecii*, because chest CT showed a diffuse ground glass appearance.

Despite our aggressive treatment, septic shock developed, accompanied with arrhythmia and severe upper gastrointestinal bleeding. She expired on the 120th admission day.

Discussion

To the best of our knowledge, this is the first report of coexistent invasive pulmonary aspergillosis and active pulmonary TB in a patient with ESRD in Taiwan. Invasive pulmonary aspergillosis is an opportunistic infectious disease, often occurring in patients who are very severely immunocompromised, but occasionally in immunocompetent patients. A large-scale autopsy study on the causes of death in a tertiary hospital in India demonstrated that 0.19% of patients died of invasive pulmonary aspergillosis; their ages ranged from 5 months to 67 years. Besides dyspnea, fever, cough with mucopurulent expectoration, chest pain and hemoptysis were common symptoms, but 41% had no respiratory symptoms at all [7].

The main predisposing factors were prolonged and severe neutropenia, allogeneic or autologous hematopoietic stem cell transplantation, solid organ transplantation, steroid therapy, potent immunosuppressive therapy, advanced acquired immune deficiency syndrome, and chronic granulomatous disease [1].

CT of the chest is more sensitive than a radiograph for the detection of early invasive pulmonary aspergillosis and should be considered in patients with 10 to 14 days of neutropenia (neutrophil count <500 per cubic millimeter) and persistent or recurrent fever of unknown cause that is unresponsive to empirical antibacterial agents. The earliest radiologic sign is a nodule. Other radiographic findings include the "CT halo sign", consolidation, wedge-shaped infarcts and cavitation [2].

Laboratory diagnostic methods for pulmonary invasive aspergillosis include sputum culture, bronchoalveolar culture, the serum galactomannan test, serum beta-D-glucan, polymerase chain reaction-based detection of aspergillosi applied to blood and bronchial alveolar lavage, and invasive procedures, for example, percutaneous CT-guided lung biopsy [1].

Although it has high specificity, the sensitivity of the serum galactomannan test was only 42% in one study [8], and it showed negative results for our patient, as well. However, in a patient who is at high risk for invasive pulmo-

nary aspergillosis and has a compatible radiologic lesion (e.g., nodules or infiltrates), a positive serum galactomannan assay or culture of an *Aspergillus* species from respiratory secretions provides strong evidence of invasive pulmonary aspergillosis and can avert the need for invasive procedures such as CT-guided aspiration.

Old pulmonary TB is 1 of the precipitating factors for pulmonary *Aspergillus* colonization. Panda *et al*. [9] performed an autopsy study and showed that patients with tissue colonization with *Aspergillus* often had been treated as having pulmonary TB. It was observed that 11% of residual pulmonary cavities had *Aspergillus* colonization, and most of them were aspergillomas. Thus, TB may lead to *Aspergillus* colonization. However, pulmonary TB is not a risk factor for invasive aspergillosis. Therefore, coexisting invasive aspergillosis and pulmonary TB has rarely been reported [10-11].

Patients on hemodialysis had an age-adjusted incidence ratio for fungal infections of 9.8 compared to the general population [4]. The most common fungal infection in such patients was candidiasis (79%), followed by cryptococcosis (6%), coccidioidomycosis (4%) and aspergillosis [4, 12]. The risk of ESRD patients developing TB is 10 to 25.3-fold higher than that of healthy individuals. The prevalence of latent TB infection (LTBI) in ESRD patients ranges from 11.3% to 63.8%. Active TB disease in ESRD patients is often extrapulmonary (50-85%) and difficult to diagnose clinically [6]. So, coexistent invasive pulmonary aspergillosis and active pulmonary TB in ESRD is rare but possible, as seen in our patient.

Mortality from invasive pulmonary aspergillosis is very high. Poorly controlled infection may lead to extension to the mediastinum and chest-wall structures, and hematogenous dissemination that can involve virtually any organ. A study in the early 1990s indicated that if invasive pulmonary aspergillosis developed in bone marrow transplant recipients, the mortality rate exceeded 94%, regardless of therapy [13].

The guidelines of the Infectious Diseases Society of America recommend the use of voriconazole as the primary therapy for invasive aspergillosis [14]. Voriconazole was more effective than amphotericin B deoxycholate as initial therapy for invasive aspergillosis and was associated with significantly improved survival [2, 15].

For primary treatment of invasive pulmonary aspergillosis, intravenous or oral voriconazole is recommended for most patients. The first-line therapy is voriconazole (6 mg/kg i.v. every 12 h for 1 day, followed by 4 mg/kg i.v. every 12 h; oral dosage 200 mg every 12 h). Alternative therapy includes liposomal amphotericin B, amphotericin B lipid complex, caspofungin, micafungin, posaconazole and itraconazole [14].

In summary, we have reported the rare case of a patient with ESRD and coexistent invasive pulmonary aspergillosis and pulmonary TB. Despite starting anti-TB therapy on the 28th admission day and anti-fungal therapy (voriconazole followed by amphotericin B) on the 78th admission day after CT-guided biopsy, the patient succumbed. In countries where the prevalence of TB is high, patients with ESRD may have coexisting pulmonary TB and invasive pulmonary aspergillosis, and the outcome is often fatal.

Acknowledgement

We appreciated the assistance of Mr. Kun-Mu Lee, Department of Laboratory Medicine,

Kaohsiung Medical University Hospital.

References

1. Segal BH and Walsh TJ. Current approaches to diagnosis and treatment of invasive aspergillosis. Am J Respir Crit Care Med 2006; 173: 707-17.
2. Segal BH. Aspergillosis. N Engl J Med 2009; 360: 1870-84.
3. Collins AJ: Chapter 12 international comparison. United States renal data system (USRDS), 2009 annual data report, Volume two, National Institutes of Health, National Institute of Diabetes and Digestive and Kidney Diseases, United States, 2009; 348-50. http://www.usrds.org/2009/slides/indiv/index_esrd.html
4. Abbott KC, Hypolite I, Tveit DJ, *et al.* Hospitalizations for fungal infections after initiation of chronic dialysis in the United States. Nephron. 2001; 89: 426-32.
5. Kuo HS, Shi WY, Lin T, *et al*. Taiwan Tuberculosis Control Report, Centers for Disease Control, Department of Health, R.O.C. 2009; 17-25.
6. Lee SS, Chou KJ, Su IJ, *et al*. High prevalence of latent tuberculosis infection in patients in end-stage renal disease on hemodialysis: comparison of Quanti FERON-TB GOLD, ELISPOT, and tuberculin skin test. Infection 2009; 37: 96-102.
7. Vaideeswar P, Prasad S, Deshpande JR. *et al*. Invasive pulmonary aspergillosis: A study of 39 cases at autopsy. J Postgrad Med 2004; 50: 21-6.
8. Meersseman W, Lagrou K, Maertens J, *et al*. Galactomannan in bronchoalveolar lavage fluid, A tool for diagnosing aspergillosis in intensive care unit patients. Am J Respir Crit Care Med 2008; 177: 27-34.
9. Panda BN, Rosha D, Verma M. Pulmonary tuberculosis: a predisposing factor for colonising and invasive aspergillosis of lungs. Ind J Tub 1998; 45: 211-22.
10. Kumar AA, Shantha GP, Jeyachandran V, *et al*. Multidrug-resistant tuberculosis coexisting with aspergilloma and invasive aspergillosis in a 50-year-old diabetic woman: a case report. Cases J 2008; 8: 303-6.
11. Kueh YK, Chionh SB, Ti TY, *et al*. Tuberculosis and invasive pulmonary aspergillosis in a young woman with a myelodysplastic syndrome. Singapore Med J 1995; 36: 107-9.
12. Gandhi BV, Bahadur MM, Dodeja H, *et al*. Systemic fungal infections in renal diseases. J Postgrad Med 2005; 51: S30-6.
13. Denning DW, Stevens DA. Antifungal and surgical treatment of invasive aspergillosis: review of 2,121 published cases. Rev Infect Dis 1990; 12: 1147-201.
14. Walsh TJ, Anaissie EJ, Denning DW, *et al*. Treatment of aspergillosis: clinical practice guidelines of the Infectious Diseases Society of America. Clin Infect Dis 2008; 46: 327-60.
15. Herbrecht R, Denning DW, Patterson TF. Voriconazole versus amphotericin B for primary therapy of invasive aspergillosis. N Engl J Med 2002; 347: 408-15.

一位末期腎衰竭血液透析病患同時合併感染侵入性肺麴菌病及活動性結核病

吳大緯* 楊志仁*,** 蔡英明* 黃吉志*,*** 黃明賢*,** 王東衡*,***

侵入性肺麴菌病是最具侵略性的黴菌感染之一，常發生於嚴重免疫功能不全的病患，如嚴重持續嗜中性球數目減少、使用類固醇、血液幹細胞及其它器官移植患者，但在血液透析的病人亦容易得到黴菌感染。台灣之末期腎臟病盛行率很高，同時也是肺結核盛行區，故有可能在血液透析病人發生侵入性肺麴菌病合併肺結核感染。

一名77歲老婦人接受血液透析至今已一年半，因為發高燒、咳嗽及左上臂瘻管局部疼痛至本院求診。最初胸部X光片顯示左側肺葉實質化，同時併發大量滲出性胸水，痰液抗酸性染色亦呈現陽性，因而開始使用抗肺結核藥物，稍後痰液結核菌培養亦證實肺結核感染。

然而即使在抗結核病藥物使用下，病患仍然持續發燒。後續的胸部X光片及電腦斷層都發現肺部多處實質化陰影及雙側毛玻璃狀變化，電腦斷層導引下肺部切片組織學顯示麴菌存在，檢體培養證實薰煙麴菌 (*Aspergillus fumigatus*) 感染。先後用過各種抗黴菌藥物如Voriconazole、Amphotericin B及Caspofungin皆無效，病患仍因為敗血性休克惡化而辭世。這可能是國內第一例報導血液透析病患同時感染侵入性肺麴菌病及活動性肺結核病。早期診斷及治療對病患存活是極為重要的關鍵。***(胸腔醫學 2010; 25: 238-244)***

關鍵詞：侵入性肺麴菌病，肺結核，末期腎衰竭

高雄醫學大學附設中和紀念醫院 內科部 胸腔內科*，高雄醫學大學 醫學院 醫學系**
高雄醫學大學 醫學院 呼吸治療學系***
索取抽印本請聯絡：王東衡醫師，高雄醫學大學附設中和紀念醫院 內科部 胸腔內科，高雄市三民區自由一路100號

Complete Resection of a Huge Pleural Solitary Fibrous Tumor 30 Years after Initial Presentation

Mong-Wei Lin, Hsao-Hsun Hsu, Yung-Chie Lee

Solitary fibrous tumor of the pleura is a mesenchymal neoplasm that involves the pleura. Because the tumors do not show conventional radiological signs of malignancy and some of them are asymptomatic, a preoperative diagnosis can be difficult and referral for surgery is often delayed. We described a 67-year-old female with a huge pleural solitary fibrous tumor. The tumor was first noted 30 years ago, with a biopsy result that revealed no malignancy. She had been regularly followed up for 10 years, but then was lost. The tumor occupied the whole left pleural cavity with compression of the heart and contralateral lung, and was completely excised through 2 separate thoracotomies. No recurrence was noted after a 1-year follow-up. ***(Thorac Med 2010; 25: 245-250)***

Key words: solitary fibrous tumor, pleural tumor

Case Report

A 67-year-old female, a non-smoker with no systemic diseases, was brought to our emergency department having had a drowsy state of consciousness for 2 days. On physical examination, she had a temperature of 38.1°C (100.3°F), blood pressure of 119/69 mmHg, pulse rate of 94 beats/min, respiratory rate of 18 breaths/min, and a room air oxygen saturation of 94%. Left hemithorax breathing sounds had disappeared. Chest X-ray (CXR) showed a complete white-out of the left chest hemithorax (Figure 1A). The trachea, heart, and mediastinal structures were deviated to the right side. Chest computed tomography (CT) revealed a huge, well defined, 20 cm diameter tumor in the left pleural cavity (Figure 1B). The tumor did not invade the chest wall or adjacent organs. The left lung was consolidated and compressed by the tumor, and the mediastinum was shifted to the right side. A large amount of pleural effusion was also noted. The patient developed respiratory distress and was intubated. Blood gas data revealed respiratory acidosis (pH level: 7.216, $PaCO_2$: 106 mmHg). Thoracocentesis was performed, and 1000 c.c. of red, exudative fluid was drained (RBC: 30000/μL, WBC: 200/μL).

Tracing her previous medical records, a symptomless left lung tumor was first noted 30 years ago during a health exam (Figure 2A). The tumor was a well-defined rounded mass,

Department of Surgery, National Taiwan University Hospital and National Taiwan University College of Medicine, Taipei, Taiwan
Address reprint requests to: Dr. Yung-Chie Lee, Department of Surgery, National Taiwan University Hospital, 7 Chung-Shan South Rd., Taipei 10002, Taiwan, ROC

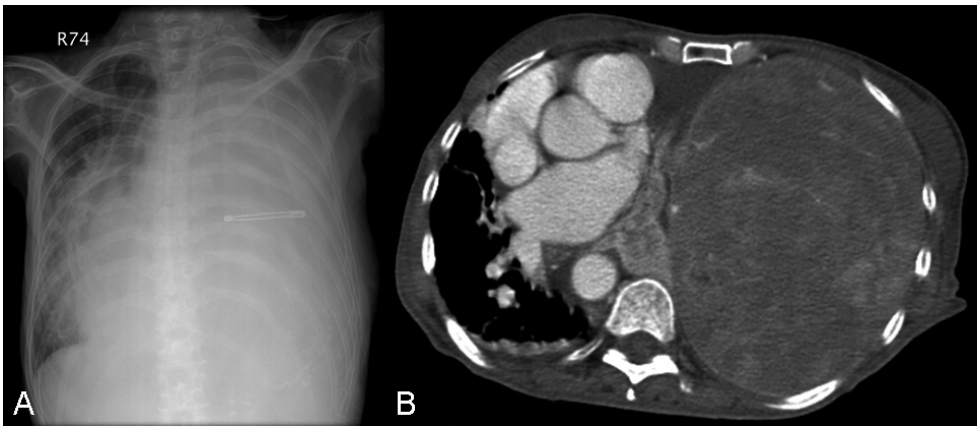

Fig. 1. (A) CXR demonstrated a complete white-out of the left chest hemithorax, 30 years after initial presentation. The trachea, heart, and mediastinal structures were deviated to the right side. The left costophrenic angle became blurred. (B) Chest CT demonstrated a well-defined tumor, 20 cm in diameter, in the left pleural cavity. The tumor did not invade the chest wall or adjacent organs. The left lung was consolidated and compressed by the tumor, and the mediastinum was shifted to the right side. A large amount of pleural effusion was also noted.

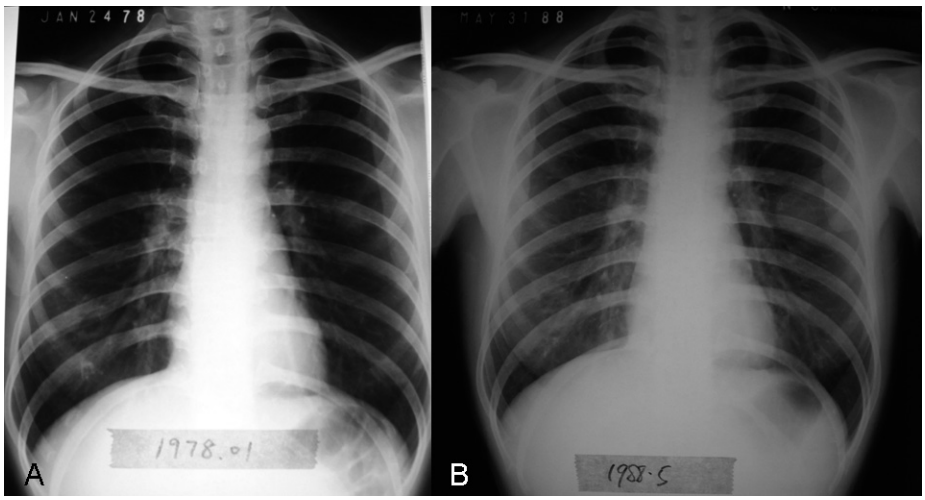

Fig. 2. (A) Thirty years before surgery, CXR demonstrated a well-defined, rounded, heterogenous tumor, 2 cm in diameter and located at the left lung field. (B) CXR demonstrated a mildly enlarged tumor after 10 years of follow-up. The shape of the tumor was still well-defined.

2 cm in diameter, and located at the left lung field. She underwent an echo-guided biopsy at a local hospital, and the result revealed no malignancy. She had received a regular follow-up for 10 years (Figure 2B). The tumor size was mildly enlarged, but still demonstrated benign radiologic features. She was then lost to follow-up. Four years ago, chronic dry cough developed, but she did not pay much attention to it. Progressive exertional dyspnea was noted during the most recent year, and the symptoms could be mildly relieved by lying in the left decubitus position.

The clinical history and image findings

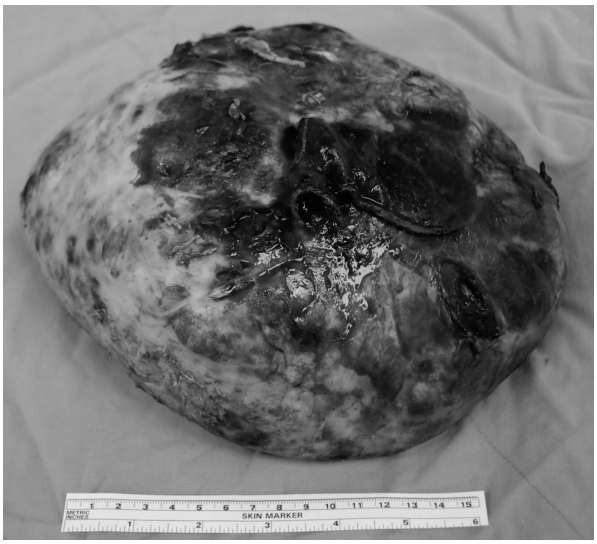

Fig. 3. The giant SFTP was well circumscribed, firm, and with focal necrosis on the cut surface. The tumor originated from the visceral pleura of the left lower lobe.

tumor was 22×18×11 cm in size, weighed 2090 gm, was well circumscribed, and had originated from the parietal pleura of the left lower lobe and occupied the whole left chest cavity (Figure 3). The tumor did not invade the chest wall, lung, diaphragm, or mediastinal structure. We performed a second thoracotomy via the 9th intercostal space to approach the lower part of the huge tumor. Microscopic examination showed a solitary fibrous tumor with a typical patternless pattern, focal myxoid change, and small foci of necrosis. Positive immunoreaction to CD34 and vimentin, but negative to SMA, was demonstrated with occasional mitosis, and a benign solitary fibrous tumor of the pleura (SFTP) was

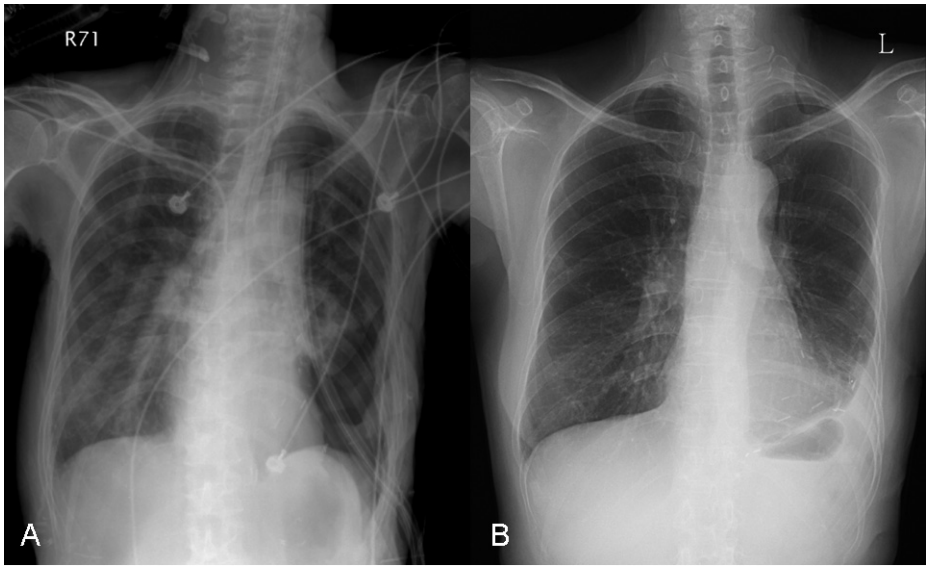

Fig. 4. (A) CXR demonstrated the consolidated left lower lobe on POD 1. (B) The left lower lobe fully expanded at the time of discharge.

demonstrated a slow-growing pleural tumor on the mediastinal structure, with a mass effect and benign behavior. Under the presumptive diagnosis of a benign pleural tumor, it was completely excised through two thoracotomies via the 5th and 9th intercostal spaces. The huge diagnosed.

Due to long-term external compression, the left lower lobe lung was consolidated after operation (Figure 4A). Re-expansion pulmonary edema developed on the 2nd postoperative day (POD 2), and subsided gradually. The patient

was extubated on POD 10. The chest tube was removed on POD 14, and she was discharged thereafter. The consolidated left lower lung fully expanded before discharge (Figure 4B). She was regularly followed up at our out-patient clinic after discharge. Neither respiratory symptoms nor recurrence were noted after 1 year of follow-up.

Discussion

SFTP is a slow-growing mesenchymal neoplasm that involves the pleura, and accounts for 5% of all pleural neoplasms [1]. It mainly affects patients in the 4^{th}-7^{th} decades, with equal gender distribution [2-3]. The symptoms of SFTP can be categorized as intrathoracic, such as dyspnea, chest pain, and hemoptysis, and systemic, such as hypoglycemia and hypertrophic pulmonary osteoarthropathy. However, half of the patients are asymptomatic at the time of diagnosis [3]. SFTP is usually first identified on CXR as a well-defined, homogeneous, rounded tumor. Pleural effusion affects 16% of these patients, with a higher prevalence in malignant SFTP patients [4]. Chest CT also demonstrates the benign features of well-delineated, homogeneous pleural tumors. Preoperative biopsy usually fails to provide a result because of the combined acellular and hypercellular portions of SFTP; therefore, it has been proven to be of little diagnostic value [2-4]. The nonspecific symptoms and benign radiologic features lead to a delayed referral for surgery. The poor accuracy of biopsy also makes it difficult to determine the time to operate. Kohler *et al*. reported that surgery was delayed for more than 6 months in 26% of patients (median 42, range 7-156 months) [5].

En bloc tumor excision is the mainstay of treatment, and the goal is complete tumor resection. A safe margin of 1~2 cm is recommended. Concomitant chest wall excision, lung lobectomy, or sleeve lobectomy may be required if the tumor invades the adjacent structures [2]. For a huge SFTP that occupies the whole chest cavity, an additional thoracotomy via the 9^{th} intercostal space may be helpful to dissect the lower part of the tumor [6]. Recurrence is not uncommon in SFTP, no matter whether benign or malignant SFTP. The overall disease-free survival rate was 95.7% in benign tumors and 67.1% in malignant tumors [1]. Radiologic examination every 6 months for 2 years after surgery and then annually was suggested [2]. In cases with recurrence, surgical resection is still the treatment of choice. The role of chemotherapy or radiotherapy is still unclear, but these 2 modalities remain as postoperative adjuvant therapy if the SFTP is malignant and recurrence is noted after surgery [2].

Our case demonstrated the slow-growing characteristic of benign SFTP. Such a long-term preoperative course, as in our case, has not been reported before. The tumor remained 2~3 cm in size during the first 10 years, and then enlarged to 22 cm and occupied the whole left chest cavity in the latter 20 years. Our experience suggests that surgery may be necessary during the early clinical stage of these pleural tumors. Video-assisted thoracoscopic surgery is advantageous in terms of a shorter hospital stay, less tissue injury, and better cosmetic results, and is the treatment of choice nowadays.

During the operation, the left lower lobe of the lung could be mildly re-expanded after en-bloc tumor excision, but was diffusely congested due to re-expansion pulmonary edema. The consolidated left lower lobe was re-expanded on POD 2. Re-expansion pulmonary edema

persisted for almost 2 weeks, and improved gradually. Our experience suggests that the consolidated lung can expand, even after such a long-term external compression, and therefore can be preserved during surgery.

In summary, our case demonstrated the slow-growth rate of benign SFTP and the long delay before referral for surgery. The symptomless and non-specific benign images features may lead to a delay of surgery. Biopsy is not a reliable diagnostic tool in SFTP patients. SFTP should be regarded as a differential diagnosis of the clinically benign lung lesion, and surgery is the treatment of choice. Life-long follow-up is suggested, no matter whether the patient received surgery or not.

References

1. Cardillo G, Carbone L, Carleo F, *et al*. Solitary fibrous tumors of the pleura: an analysis of 110 patients treated in a single institution. Ann Thorac Surg 2009; 88: 1632-7.
2. de Perrot M, Fischer S, Bründler MA, *et al*. Solitary fibrous tumors of the pleura. Ann Thorac Surg 2002; 74: 285-93.
3. Sung SH, Chang JW, Kim J, *et al*. Solitary fibrous tumors of the pleura: surgical outcome and clinical course. Ann Thorac Surg 2005; 79: 303-7.
4. England DM, Hochholzer L, McCarthy MJ. Localized benign and malignant fibrous tumors of the pleura. A clinicopathologic review of 223 cases. Am J Surg Pathol 1989; 13: 640-58.
5. Kohler M, Clarenbach CF, Kestenholz P, *et al*. Diagnosis, treatment and long-term outcome of solitary fibrous tumours of the pleura. Eur J Cardiothorac Surg 2007; 32: 403-8.
6. Hu CK, Chang YL, Lin WC, *et al*. Resection of a giant thoracic solitary fibrous tumor through two separate thoracotomies. J Thorac Cardiovasc Surg 2008; 136: 1077-9.

巨大肋膜腔單發性纖維瘤之三十年病程及完整手術切除

林孟暐　徐紹勛　李元麒

肋膜腔單發性纖維瘤是一種間葉細胞起源的肋膜腫瘤。這類腫瘤常常沒有症狀，影像學檢查常為良性表現，因此較難在手術前診斷，接受手術治療的時間也因而常常延誤。本文描述一位巨大肋膜腔單發性纖維瘤病人，這位六十七歲的女性病人三十年前即發現左側的肺部腫瘤，因切片結果顯示沒有惡性細胞，追蹤十年以後即沒有再回診。三十年後再來到急診處時，腫瘤已佔滿整個左側胸腔，壓迫到心臟及對側的肺葉，並導致呼吸衰竭。這個巨大的肋膜腔單發性纖維瘤順利地經由側面胸廓切開術式完整切除。追蹤一年後沒有復發的情形。*(胸腔醫學* ***2010; 25: 245-250****)*

關鍵詞：單發性纖維瘤，肋膜腫瘤

國立台灣大學附屬醫院　外科部
索取抽印本請聯絡：李元麒醫師，國立台灣大學附屬醫院　外科部，台北市中山北路1段7號

Fulminating Pneumococcal Pneumonia with Acute Respiratory Distress Syndrome in a Healthy Young Patient Following Pandemic (H1N1) 2009 Influenza

Tung-Yang Wu*,**, Wann-Cherng Perng**, Kao-Yao Chang*, Chien-Wen Chen**

Secondary bacterial pneumonia developing after (H1N1) 2009 influenza infection was an important cause of influenza-associated death. We report the case of a 23-year-old previously healthy soldier who was initially diagnosed with influenza A infection. Three days later, the disease progressed, pneumonia developed in the left upper and lower lobes, and respiratory failure was imminent, despite oseltamivir therapy. The diagnosis of secondary pneumococcal pneumonia after 2009 H1N1 infection was made on the basis of positive results for 2009 H1N1 influenza in the real-time reverse-transcriptase polymerase chain reaction performed on a nasal swab, and in the urinary pneumococcal antigen test. The patient was successfully treated using oxygen mask supplementation and antiviral and antibiotic therapies. In immunocompetent patients with confirmed influenza A infection, secondary bacterial infection should be considered when respiratory symptoms progress, even after standard management. The rapid progression of community-acquired pneumonia accompanied with respiratory distress syndrome is a potentially fatal complication occurring secondary to (H1N1) 2009 influenza infection. ***(Thorac Med 2010; 25: 251-257)***

Key words: pandemic (H1N1) 2009 infection, pneumococcal pneumonia, respiratory failure

Introduction

In April 2009, (H1N1) 2009 infection was first detected in the United States, and then spread rapidly worldwide. As of 24 January 2010, 14,711 deaths had been reported to the World Health Organization (WHO). [1] Secondary bacterial pneumonia associated with influenza, including that caused by (H1N1) 2009 infection, has a high mortality rate if diagnosed late or misdiagnosed. [2-4] Early treatment of the predisposing or concomitant viral illness ameliorates subsequent bacterial complications and increases the survival rate. Herein, we present a case of secondary pneumococcal pneumonia after (H1N1) 2009 infection; the pneumonia had a fulminating course with acute respiratory distress syndrome (ARDS).

* Department of Internal Medicine, Kaohsiung Armed Forces General Hospital, Kaohsiung, Taiwan; ** Division of Pulmonary and Critical Care, Tri-Service General Hospital, Taipei, Taiwan
Address reprint requests to: Dr. Chien-Wen Chen, Division of Pulmonary and Critical Care, Tri-Service General Hospital, National Defense Medical Center, No. 325, Section 2, Cheng-Kung Road, Nei-Hu 114, Taipei, Taiwan

Case Report

A 23-year-old previously robust soldier with a body mass index (BMI) of 21 kg/m^2, presented to the emergency department with generalized weakness, productive cough, and fever that had persisted for 1 week. Three days earlier, a rapid influenza diagnostic test performed at a local clinic had yielded positive results, so he was initially prescribed oseltamivir (75 mg, twice a day). He had a productive cough with bloody and yellowish sputum and respiratory distress, and was admitted to our hospital for aggressive management.

On physical examination, the following results were obtained: blood pressure, 124/78 mmHg; pulse rate, 112 beats per minute; respiratory rate, 30-40 breaths per minute; and body temperature, 38.5°C. The patient was in respiratory distress. Rhonchi were heard in the left lung field. Laboratory tests revealed the following results: white blood cell count, 7.3 × 10^3/mm^3 with 98.1% neutrophils; hemoglobin level, 14.6 g/dL; platelet count, 99 × 10^3/mm^3; C-reactive protein (CRP) level, 37.91 mg/dL. Arterial blood gas, FiO_2 60%, analysis revealed the following results: pH 7.444, $PaCO_2$, 33.5 mmHg; PaO_2, 57.3 mmHg; and oxygen satu-

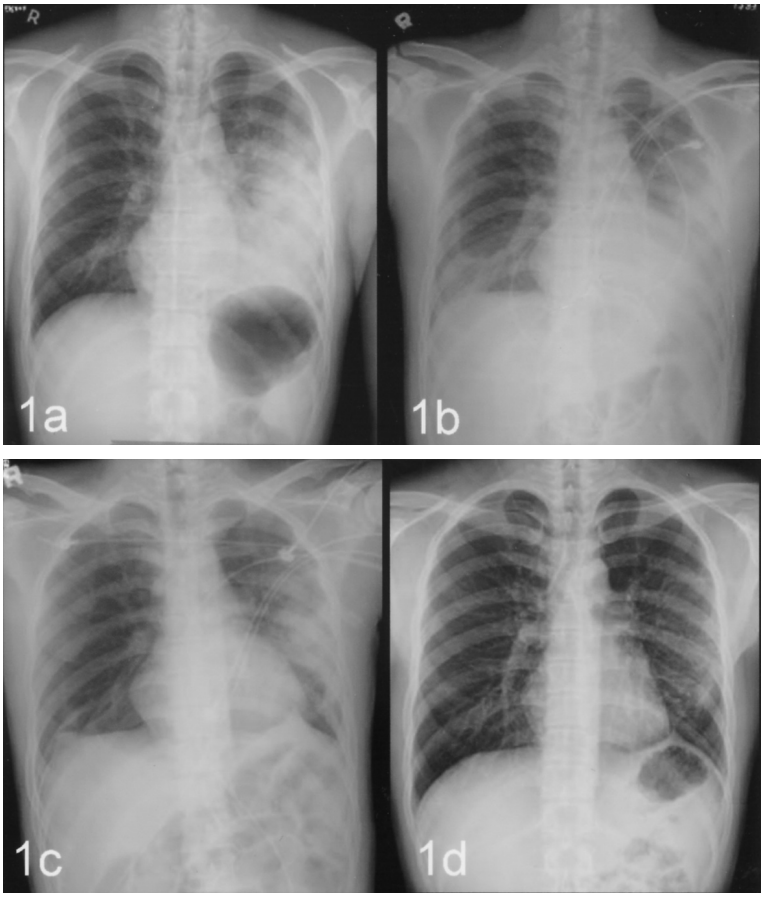

Fig. 1. (A) On admission, chest radiograph reveals a large area of patchy consolidation in the left lung field. (B) On day 3, large areas of ill-defined air-space consolidation in the left lung and a new patchy opacity in the right lower lung field can be seen. (C) On day 6, partial resolution of previous consolidation and pulmonary infiltration was revealed. (D) On day 10, a remarkable resolution of the bilateral pulmonary infiltration and consolidation can be seen.

ration, 91.4%. The remaining laboratory data were within normal limits. The chest X-ray film showed a large area of patchy consolidation in the left lung field (Figure 1a).

Moxifloxacin (400 mg) was administered intravenously once a day, and concomitant oseltamivir therapy (75 mg, twice a day) was continued. Hypoxemia was initially treated by continuous oxygen supplementation using an oxygen mask (10 L/min). A nasopharyngeal swab tested positive for (H1N1) 2009 infection in real-time reverse-transcriptase polymerase chain reaction (rRT-PCR). The pneumococcal urinary antigen test was positive, but the tests for Chlamydia, Legionella, *Pneumocystis jiroveci* pneumonia (PJP), Cytomegalovirus, and acid-fast bacilli were negative. The diagnosis was (H1N1) 2009 infection with secondary pneumococcal pneumonia and ARDS.

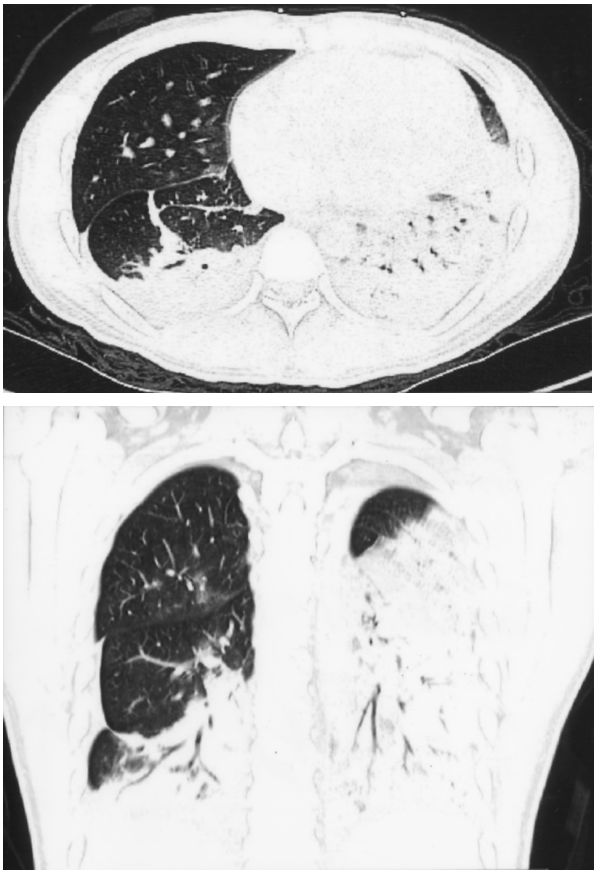

Fig. 2. Computed tomography (CT) of the chest discloses patchy areas of airspace consolidation and ground-glass opacity in both lungs, especially both lower lobes and the LUL.

On day 3, computed tomography of the chest revealed patchy consolidations and ground-glass opacities in both lower lobes and the left upper lobe (Figure 2). The patient was always alert despite the hypoxemia and respiratory distress. Further chest plain films showed a new patchy opacity in the right lower lung field (Figures 1b, 1c). Oxygen supplementation (6-10 L/min) using a mask was well tolerated, and pulse oximetry revealed oxygen saturation of approximately 90-98%. Hypercapnic respiratory failure did not occur. After a 1-week course of antibiotics and antiviral medications, the symptoms of respiratory distress, hypoxemia, and fever subsided. On day 8, the treatment was shifted to oral moxifloxacin therapy (400 mg, once a day). A chest X-ray film showed almost complete resolution of the bilateral pulmonary infiltrates (Figure 1d). He was discharged on day 13, without any sequelae.

Discussion

The (H1N1) 2009 virus can cause outbreaks of febrile respiratory infection resulting in self-limited to severe illness. In our patient, influenza-like illness was followed by lobar pneumonia during which the H1N1 PCR and urinary pneumococcal antigen test (sensitivity, 81%; specificity, 98%) [5] were positive; these results confirmed the diagnosis of community-acquired pneumococcal pneumonia occurring after the (H1N1) 2009 infection. Thus, the diagnosis was rapidly confirmed in this patient who had fortuitously presented with influenza-like symptoms at a time when (H1N1) 2009

infection had caused outbreaks associated with high mortality rates in critically ill patients with influenza-associated pneumonia.

Infection with (H1N1) 2009 may increase susceptibility to secondary bacterial infections, which in turn increase the severity of (H1N1) 2009, but microbiological data on such secondary infections have rarely been obtained. The clinical manifestations present as a biphasic illness with features of an influenza-like illness followed by a second rise in temperature or a persistent fever along with purulent sputum. [6] Secondary bacterial infection is reported to occur in approximately 4% of patients infected with (H1N1) 2009; *Streptococcus pneumoniae* and *Staphylococcus aureus* are the most commonly isolated pathogens. [2, 7-10] The risk factors for serious respiratory complications are as follows: obesity (especially morbid obesity), comorbid respiratory or cardiovascular disease, and immunosuppression. [11-12] It was of interest that no predisposing factors were observed in our patient, whose condition rapidly deteriorated to the point of ARDS. This is a rare clinical presentation, consistent with the findings of a previous study wherein coinfection with bacteria and the influenza virus was found to be more severe than independent infection with either. [2] In other words, the additive effects of the 2 diseases may predispose to a worse outcome. [13] Furthermore, secondary bacterial infection should be considered early in an (H1N1) 2009-infected patient with lobar pneumonia, despite negative bacterial pathogen cultures. The symptoms of (H1N1) 2009 infection combined with secondary bacterial infection might be misleading, resulting in a delay in antibiotic therapy use beyond the optimal time for initiation.

Our patient's condition rapidly progressed toward respiratory failure within 6 days of admission; this finding is consistent with those reported in some published papers in which the concerned patients initially had an influenza-like illness that rapidly progressed to ARDS and even respiratory failure within 5-7 days. [3, 8] In addition, we initially observed severe hypoxemia in our patient; this might be the most characteristic laboratory finding observed in intensive care unit (ICU) patients with (H1N1) 2009 infection complicated with bacterial pneumonia. [3, 8] In short, the clinical course was characterized by severe pneumonia, hypoxemia with multifocal infiltrates on chest X-ray, and rapid progression to ARDS. [14] Therefore, clinicians treating such patients should be aware of the possibility of the rapid deterioration of their respiratory symptoms. [8]

A previous study revealed that coinfection with bacteria and the influenza virus was more difficult to treat than secondary bacterial infections that occurred after a distinct period of initial recovery from influenza infection. [2] Our patient was in the former category, but the potential airway compromise was successfully prevented under intensive ICU monitoring. In line with other reports, early administration of the appropriate antibiotics combined with antiviral medications is suggested for patients with (H1N1) 2009 infection complicated with secondary bacterial pneumonia to improve what could be a poor outcome. [6, 13, 15] To our knowledge, early tracheal intubation for patients with ARDS with acute hypoxic respiratory failure is the preferred management. [16] But based on our patient's experience in treatment, it is more important to select patients properly and monitor them closely in an intensive-care setting, thus possibly avoiding the need for invasive intubation. In addition, a

significantly higher CRP level was detected in our patient; this might be a predictive factor for concomitant secondary bacterial infection with a pathogen typically observed in such cases. [17]

Early treatment of the predisposing viral illness can ameliorate subsequent bacterial complications and reduce hospital mortality associated with influenza. [2, 18] Antiviral treatment with the neuraminidase inhibitor oseltamivir within 2 days of the onset of symptoms is considered most effective for (H1N1) 2009 infection. [3-4, 19] During an influenza pandemic such as the (H1N1) 2009 pandemic, antiviral therapy should be prioritized for all patients who present with influenza-like symptoms at admission even if community-acquired pneumonia has been diagnosed and the rapid influenza test is negative. [8-9]

In conclusion, *Streptococcus pneumoniae* is one of the most common pathogens causing secondary bacterial pneumonia after (H1N1) 2009 infection, and the urinary pneumococcal antigen test might be the optimal rapid screening method. Rapid exacerbation of the respiratory symptoms accompanied by an elevated CRP level and lobar pneumonia should alert physicians to the necessity of an early detection of bacterial pneumonia in persons infected with (H1N1) 2009 influenza.

References

1. World Health Organization. Pandemic (H1N1) 2009-update. Available at: http://www.who.int/csr/don/2010_01_29/en/index.html.
2. McCullers JA. Insights into the interaction between influenza virus and pneumococcus. Clin Microbiol Rev 2006; 19: 571-82.
3. Perez-Padilla R, de la Rosa-Zamboni D, Ponce de Leon S, *et al*. Pneumonia and respiratory failure from swine-origin influenza A (H1N1) in Mexico. N Engl J Med 2009; 361: 680-9.
4. Leelarasamee A, Jongwutiwes U, Tantipong H, *et al*. Fulminating influenza pneumonia in the elderly: a case demonstration. J Med Assoc Thai 2008; 91: 924-30.
5. Boulware DR, Daley CL, Merrifield C, *et al*. Rapid diagnosis of pneumococcal pneumonia among HIV-infected adults with urine antigen detection. J Infect 2007; 55: 300-9.
6. Australian Government Department of Health and Ageing. Resource — clinical management of pandemic (H1N1) 2009. Available at: http://www.public.health.wa. gov.au/cproot/2382/2/090709%20Clinical%20Resource%20H1N1%2009%20-%20FINALGDL.pdf.
7. O'Brien KL, Walters MI, Sellman J, *et al*. Severe pneumococcal pneumonia in previously healthy children: the role of preceding influenza infection. Clin Infect Dis 2000; 30: 784-9.
8. Rello J, Rodriguez A, Ibanez P, *et al*. Intensive care adult patients with severe respiratory failure caused by Influenza A (H1N1) v in Spain. Crit Care 2009; 13: R148.
9. Dawood FS, Jain S, Finelli L, *et al*. Emergence of a novel swine-origin influenza A (H1N1) virus in humans. N Engl J Med 2009; 360: 2605-15.
10. Louie JK, Acosta M, Winter K, *et al*. Factors associated with death or hospitalization due to pandemic 2009 influenza A(H1N1) infection in California. JAMA 2009; 302: 1896-902.
11. Grasselli G, Foti G, Patroniti N, *et al*. A case of ARDS associated with influenza A - H1N1 infection treated with extracorporeal respiratory support. Minerva Anestesiol 2009; 75: 741-5.
12. Miller RR 3rd, Markewitz BA, Rolfs RT, *et al*. Clinical findings and demographic factors associated with intensive care unit admission in Utah due to 2009 novel influenza A (H1N1) infection. Chest 2009 Nov 20. Available at: http://chestjournal.chestpubs.org/content/early/2009/11/19/chest.09-2517.long
13. Karlstrom A, Boyd KL, English BK, *et al*. Treatment with protein synthesis inhibitors improves outcomes of secondary bacterial pneumonia after influenza. J Infect Dis 2009; 199: 311-9.
14. Al Hajjar S, McIntosh K. The first influenza pandemic of the 21st century. Ann Saudi Med 2010; 30: 1-10.
15. Charles PG, Johnson PD, Collignon PJ. Can we readily identify patients who need antibiotics in a severe influ-

enza pandemic? Med J Aust 2009; 191: 517-8.
16. Agarwal R, Handa A, Aggarwal AN, *et al*. Outcomes of noninvasive ventilation in acute hypoxemic respiratory failure in a respiratory intensive care unit in north India. Respir Care 2009; 54: 1679-87.
17. Kruger S, Ewig S, Papassotiriou J, *et al*. Inflammatory parameters predict etiologic patterns but do not allow for individual prediction of etiology in patients with CAP: results from the German competence network CAPNETZ. Respir Res 2009; 10: 65.
18. Alonso-Tarres C, Cortes-Lletget C, Pintado S, *et al*. Severe influenza A (H1N1) v in patients without any known risk factor. Crit Care 2009; 13: 425.
19. Gilsdorf A, Poggensee G. Influenza A (H1N1) v in Germany: the first 10,000 cases. Euro Surveill 2009; 14: 1-4.

一個感染2009新型流感的健康年輕病患併發猛暴性的鏈球菌肺炎伴隨急性呼吸窘迫症候群的案例報告

吳東陽*,** 彭萬誠** 張高耀* 陳健文**

在2009新型流感感染期間併發續發性的細菌性肺炎是一個導致新型流感死亡的重要原因。在此我們報告一位23歲的健康軍人，一開始診斷出A型流感的感染，經投予抗病毒藥物治療，三天之後仍併發持續惡化的大葉性肺炎伴隨瀕臨插管的呼吸衰竭，最後經由陽性的2009新型流感聚合連鎖反應分析（PCR）及尿液肺炎球菌抗原篩檢證實為2009新型流感的感染併發續發性的鏈球菌肺炎，之後成功地以氧氣面罩供應氧氣、加上抗病毒藥物合併適當的抗生素治療解決其問題。由此提醒我們，在一個免疫功能健全的病患身上，若證實有A型流感的感染並接受標準的抗病毒藥物治療之後，仍發現呼吸道症狀有持續惡化的情形時，要考慮是否有續發性的細菌感染，因為在感染2009新型流感之後續發快速惡化的社區性肺炎伴隨呼吸窘迫症狀是一個潛在致命的併發症。*(胸腔醫學* ***2010; 25: 251-257)***

關鍵詞：2009新型流感，鏈球菌肺炎，呼吸衰竭

國軍高雄總醫院 內科部*，三軍總醫院 胸腔內科**
索取抽印本請聯絡：陳健文醫師，三軍總醫院 胸腔內科，台北市內湖區成功路二段325號

Pulmonary Amyloidosis Presenting as a Solitary Pulmonary Nodule in a Patient with Sjogren's Syndrome

Chia-Cheng Liu*, Po-Kuei Hsu*,**,***, Hsin-Ju Lin****, Wen-Hu Hsu*,***,*****

A 41-year-old woman was admitted with a 10-month history of generalized skin itch, dry eye and dry mouth. Sjogren's syndrome was diagnosed. However, a solitary pulmonary nodule was incidentally found on routine chest radiography on admission. Computed tomography showed the lesion to be well-defined, homogenous and 1.3 cm in size. To ascertain the pulmonary pathology, wedge resection of the right lower lobe was performed. Microscopically, the lesion exhibited eosinophilic amorphous substance deposition, which showed green birefringence when stained with Congo red. Pulmonary amyloidosis with Sjogren's syndrome is rare and most cases present as multiple nodules or diffuse reticulonodular infiltrates. Solitary nodular pulmonary amyloidosis with Sjogren's syndrome is a very rare condition and may mimic pulmonary neoplasm. Surgical resection of the pulmonary nodule not only confirms the diagnosis, but also excludes the existence of malignancy. ***(Thorac Med 2010; 25: 258-262)***

Key words: pulmonary amyloidosis, Sjogren's syndrome

Introduction

Pulmonary manifestations of Sjogren's syndrome encompass a variety of presentations ranging from benign lesions to malignant lymphocytic lymphoma [1]. Pulmonary amyloidosis is rarely associated with Sjogren's syndrome and most cases present as multiple nodules or diffuse reticulonodular infiltrates [2]. Herein, we present a case of solitary nodular pulmonary amyloidosis in a patient with Sjogren's syndrome, which is a very rare condition.

Case Report

A 41-year-old woman was admitted with a 10-month history of generalized skin itch, dry eye and dry mouth. Her past medical history was unremarkable and she denied any exposure to chemicals. Physical examination revealed nothing abnormal, except dryness of the oral cavity and eye. The Schirmer's test was

* Division of Thoracic Surgery, Department of Surgery, Taipei Veterans General Hospital; ** Department of Surgery, Chutung Veterans Hospital; *** National Yang-Ming University, School of Medicine; **** Department of Pathology, Taipei Veterans General Hospital; ***** Taipei Medical University, School of Medicine, Taipei, Taiwan, R.O.C.
Address reprint requests to: Dr. Wen-Hu Hsu, Division of Thoracic Surgery, Department of Surgery, Taipei Veterans General Hospital, Taiwan, No. 201, Sec. 2, Shih-Pai Road, Taipei 112, Taiwan

positive. Routine chest radiography revealed nodular opacity in the right lower lung field. Suspected of having sicca syndrome, she underwent a sialoscintigraphy, which showed moderate xerostomia. Salivary gland biopsy showed lymphocytic infiltrates. The serological tests indicated positive antinuclear antibody with a titer of 1:160 (speckled pattern), anti-dsDNA of 11 IU/ml (normal <30 IU/ml), rheumatoid factor of <10 IU/ml (normal <40 IU/ml), anti-Ro antibody (SSA) of >240 (normal <7 IU/ml), anti-Ra antibody (SSB) of 16.3 U/ml (normal <7 IU/ml), and normal C3, C4, IgG, IgA, IgM, CRP and ESR. The diagnosis of Sjogren's syndrome was established and she was given methylprednisolone pulse therapy (intravenous 1000 mg), followed by oral hydroxychloroquine 200 mg twice daily and oral methylprednisolone 4 mg daily by a rheumatologist.

The patient was then referred to a thoracic surgeon for evaluation of the pulmonary nodule that had been incidentally found. Computed tomography (CT) depicted a 1.3-cm well-defined homogenous pulmonary nodule at the right lower lobe (Figure 1). The CEA level was 1.74 ng/ml (normal <6 ng/ml). Histochemical examination of the specimen obtained by CT-guided percutaneous biopsy revealed chronic inflammation with mucoid material. To ascertain the pulmonary pathology, the patient underwent further surgical intervention. Wedge resection of the right lower lobe was performed. A 1.7 × 1.2 × 1.2 cm, firm, well-circumscribed yellowish nodule was noted grossly. The lesion

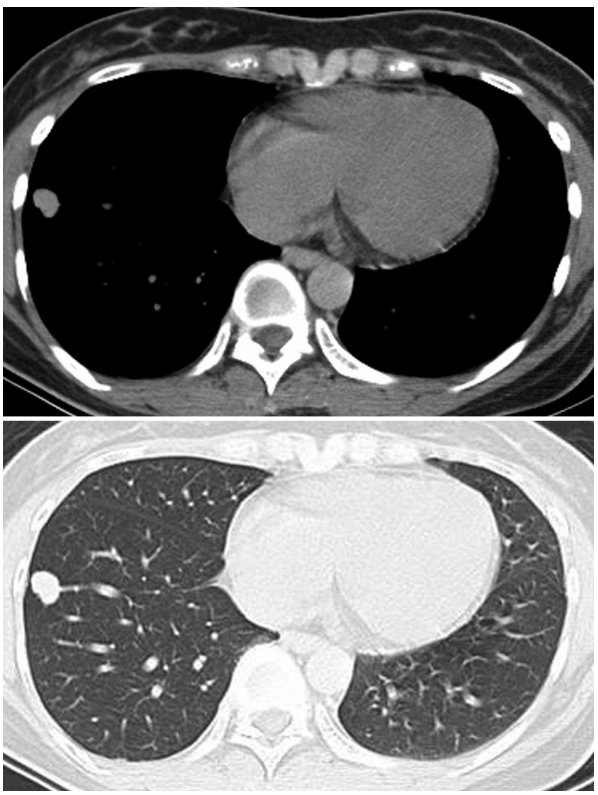

Fig. 1. Computed tomography depicts a well-defined, homogenous, non-calcified pulmonary nodule at the right lower lobe.

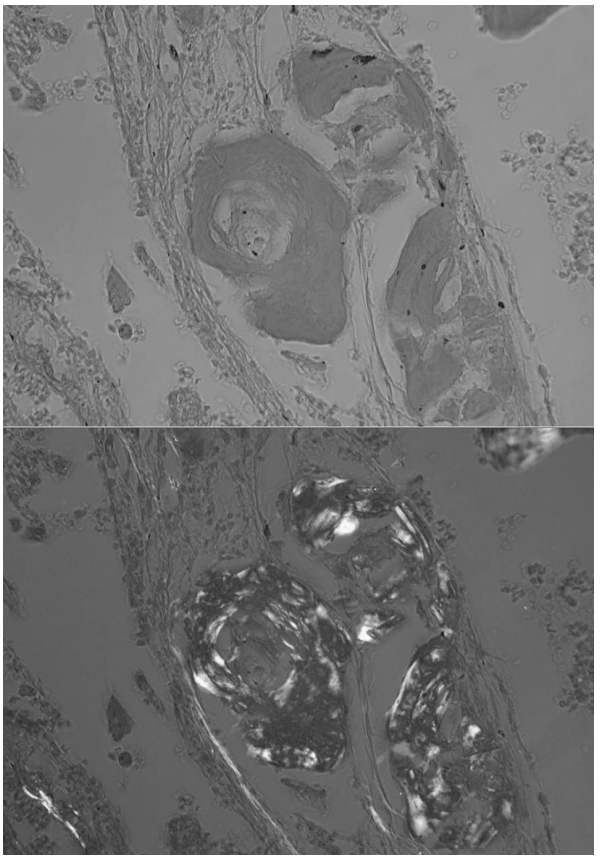

Fig. 2. Congo red stain (x200) under polarized light reveals green birefringence in the amorphous substance as well as the vessel wall, consistent with an amyloid deposit.

exhibited eosinophilic amorphous substance deposition microscopically, accompanied with a multinucleated giant cell reaction. Congo red stain under polarized light revealed green birefringence in the amorphous substance, as well as the vessel wall, which was consistent with amyloid deposits (Figure 2). She was discharged with a diagnosis of nodular pulmonary amyloidosis with Sjogren's syndrome. One year after operation the patient was well with no new pulmonary lesion.

Discussion

Amyloidosis is characterized by deposition of extracellular insoluble amyloid fibrils, which contain a cross-β structure. When stained with Congo red, the amyloid produces a pathognomonic green birefringence under polarized light, which is the gold standard in diagnosis [3]. The classification of amyloidosis is based on the precursor proteins. Whereas primary amyloidosis (AL type) consists of fragments of immunoglobulin, secondary amyloidosis (AA type) is derived from serum amyloid A, which is an acute phase protein produced in an inflammatory condition [4]. Amyloid deposits can be present in almost every part of the body and cause a wide range of tissue dysfunction [3].

In 1877, Lesser first reported amyloidosis localized to the lower respiratory tract [5]. So far, amyloidosis of the respiratory tract has been recognized in 4 typical patterns: tracheobronchial, nodular parenchymal, diffuse alveolar septal and lymphadenopathy, based on CT exam [4]. Nodular pulmonary amyloidosis is usually incidentally found on routine examination. The nodules usually have a well-defined margin and a peripheral or subpleural distribution. The right lower lobe is the most affected site [6]. The average age at presentation is the 6th decade of life and there is an equal sex distribution. Most patients are asymptomatic, but hemoptysis, cough, chest pain and dyspnea have been reported [6]. Although localized pulmonary amyloid nodules are characterized by a benign course without systemic involvement, they grow slowly and may have a space-occupying effect. In an observation study by Eisenberg *et al*, a 70-year-old woman was diagnosed with nodular pulmonary amyloidosis. No specific therapy was given due to the benign nature of the amyloidosis. However, the slow-growing amyloid nodule finally occupied the entire lung field and was complicated with hemoptysis during a 14-year period [7].

Sjogren's syndrome is both an inflammatory condition and an immunological disorder. The nature of the disease may be the possible explanation that links Sjogren's syndrome and amyloidosis, which is caused by an accumulation of misfolded acute phase proteins or immunoglobulin fragments. Pulmonary amyloidosis in patients with Sjogren's syndrome is not common and a broad spectrum of lung involvement has been described, including xerotrachea, lymphocytic bronchial inflammation, lymphocytic interstitial pneumonia, organizing pneumonia, nonspecific interstitial pneumonia (NSIP), follicular or constrictive bronchiolitis, primary pulmonary lymphoma, multiple cysts and pulmonary hypertension [8]. Whereas NSIP was a major feature in the study by Shi *et al*. [8], solitary nodular pulmonary amyloidosis in a patient with Sjogren's syndrome is very rare. Sakai *et al*. reported a 58-year-old woman presenting with a solitary pulmonary nodule at the left lower lobe [9]. Nodular pulmonary amyloidosis was proved by thoracoscopic biopsy. The patient was subsequently diagnosed as having

Sjogren's syndrome. The second case, reported by Srinivas *et al*. [10], involved a 52-year-old woman with a 25-year history of Sjogren's syndrome who underwent an examination for hemoptysis. CT revealed a lobulated mass lesion at the left lower lobe. A resected specimen confirmed nodular amyloidosis. From the literature and our experience, Sjogren's syndrome with solitary pulmonary amyloidoma may occur either before or after the diagnosis of Sjogren's syndrome. On CT, the lesions are frequently found at the lower lobes and are difficult to distinguish from bronchogenic carcinoma. Although there is insufficient data regarding the appropriate therapy for nodular pulmonary amyloidosis, surgical resection is indicated for hemoptysis and the exclusion of malignancy.

In conclusion, Sjogren's syndrome associated with solitary nodular pulmonary amyloidosis is a very rare condition. Resection of the pulmonary nodule not only confirms the diagnosis but also excludes the existence of malignancy.

References

1. Strimlan CV, Rosenow EC, Divertie HB, *et al*. Pulmonary manifestations of Sjogren's syndrome. Chest 1976; 70: 354-61.
2. Wong BC, Wong KL, Ip MS, *et al*. Sjogren's syndrome with amyloid A presenting as multiple pulmonary nodules. J Rheumatol 1994; 21: 165-7.
3. Pepys MB. Amyloidosis. Annu Rev Med 2006; 57: 223-41.
4. Aylwin ACB, Gishen P, Copley SJ. Imaging appearance of thoracic amyloidosis. J Thorac Imaging 2005; 20: 41-5.
5. Lesser A. Ein Fall von Enchondroma osteoides mixtum der Lunge mit partieller Amyloidentartung. Virchow Arch 1877; 69: 404-8.
6. Hui AN, Koss MN, Hochholzer L, *et al*. Amyloidosis presenting in the lower respiratory tract. Arch Pathol Lab Med 1986; 110: 212-8.
7. Eisenberg R, Sharma OP. Primary pulmonary amyloidosis, an unusual case with 14 years' survival. Chest 1986; 89: 889-91.
8. Shi JH, Liu HR, Xu WB, *et al*. Pulmonary manifestations of Sjogren's syndrome. Respiration 2009; 78: 377-86.
9. Sakai K, Ohtsuki Y, Hirasawa Y, *et al*. Sjogren's syndrome with solitary pulmonary amyloidosis. Nihon Kokyuki Gakkai Zasshi 2004; 42: 330-5.
10. Srinivas P, Liam CK, Jayaram G. Localized nodular pulmonary amyloidosis in a patient with sicca syndrome. Med J Malaysia 2000; 55: 385-7.

在修格連氏症候群病人上以單一肺結節表現的類澱粉沉積症

劉佳政* 徐博奎*,**,*** 林心如**** 許文虎*,***,*****

一位41歲女性以十個月之久的皮膚癢，口乾及眼乾表現，診斷為修格連氏症候群後，胸部X光發現一孤立性肺結節，胸部電腦斷層顯示一邊緣規則且均質，大小約1.3公分的病灶，為排除惡性腫瘤，病人接受局部肺切除。顯微鏡下顯現嗜伊紅性不規則物質沉積，剛果紅染色下有綠色雙折射現象。肺部類澱粉沉積合併修格連氏症候群實屬罕見，且大多案例以多發性結節或廣泛性網目斑點狀浸潤，以孤立性肺結節表現的肺部類澱粉沉積合併修格連氏症候群是非常少見，且影像學常可能類似癌症表現，手術切除非但可確定診斷亦可排除癌症可能。*(胸腔醫學* ***2010; 25: 258-262)***

關鍵詞：肺部類澱粉沉積，修格連氏症候群

*台北榮民總醫院 外科部 胸腔外科，**竹東榮民醫院 外科部，***國立陽明大學 醫學系
****台北榮民總醫院 病理部，*****台北醫學院 醫學系
索取抽印本請聯絡：許文虎醫師，台北榮總 胸腔外科，台北市石牌路二段201號

Successful Repair of Complete Traumatic Tracheo-bronchial Disruption with Extra-corporeal Membrane Oxygenation Support

Ka-I Leong, Pei-Ming Huang, Wen-Je Ko*, Yung-Chie Lee

Complete tracheo-bronchial disruption following blunt chest trauma is rare. The prognosis is poor, with almost 80% of patients dying at the scene of injury. Successful treatment requires a high level of alertness and early surgical repair. At the same time, providing adequate oxygenation and maintaining stable hemodynamics are frequently difficult in these types of airway injuries. We reported the case of a 47-year-old man with an anterior chest wall crush injury who was given extra-corporeal membrane oxygenation (ECMO) support in the management of a completely transected right main bronchus and ruptured trachea following blunt chest trauma. Post-operative bronchoscopic examination showed good healing with no stricture, and the patient was asymptomatic 18 months after surgery. ECMO is used for oxygen supplementation during reconstruction in many traumatic lung injury and pediatric tracheal stenosis patients. Good survival and outcomes have been noted in the medical literature. Systemic tissue oxygenation and cardio-pulmonary support can be maintained during the peri- and post-operative period via the extra-corporeal circuit to minimize lung barotrauma from prolonged high positive pressure. In our case, ECMO was successfully used in a patient with bronchial transection to provide adequate oxygen supplementation and tissue perfusion before and after surgery. ***(Thorac Med 2010; 25: 263-267)***

Key words: tracheo-bronchial disruption, extra-corporeal membrane oxygenation

Introduction

Complete tracheo-bronchial disruption following blunt chest trauma is rare. The prognosis is poor, with almost 80% of patients dying at the scene of injury [1]. Successful treatment requires a high level of alertness and early surgical repair. At the same time, providing adequate oxygenation and maintaining stable hemodynamics are frequently difficult in patients with these types of airway injuries. Herein, we report a case of using extra-corporeal membrane oxygenation (ECMO) support in the management of a completely transected right main bronchus and ruptured trachea following blunt chest trauma.

Division of Thoracic Surgery, Department of Surgery; *Department of Traumatology, National Taiwan University Hospital and National Taiwan University College of Medicine, Taipei, Taiwan
Address reprint requests to: Dr. Yung-Chie Lee, Division of Thoracic Surgery, Department of Surgery, National Taiwan University Hospital and National Taiwan University College of Medicine, No. 7, Chung Shan S. Rd., Taipei 100, Taiwan

Case Report

The anterior chest wall of a 47-year-old man was accidentally crushed by a heavy machine around 8:44 am at his work place. When he was sent to the emergency department near his work at 9:10 am, he was suffering from severe respiratory distress with a massive air leak from the right chest tube noted during cardiopulmonary resuscitation. Bronchoscopy showed rupture of the right main bronchus, so single-lung ventilation into the left main bronchus was instituted under bronchoscopic guidance. However, the blood oxygen saturation was around 80%, even with 100% inspiratory oxygen.

The chest roentgenogram showed right pneumothorax, subcutaneous and mediastinal emphysema, and a "fallen lung" sign (lung collapse towards the lateral chest wall) on the right side (Figure 1). There were also fractures in the upper thoracic area involving the clavicles, scapula, and ribs. Chest computed tomography (CT) demonstrated deformation of the right main bronchus with specific evidence of tracheo-bronchial injury (Figure 2).

The patient was transferred to our emergency room at 1:50 pm. and his vital signs were: heart rate of 138/min, blood pressure 101/60 mmHg, and respiratory rate 20/min; arterial blood gases showed: pH: 7.010, PaO_2: 62 mmHg, $PaCO_2$: 81 mmHg, and $PaCO_2$: 25.4 mmHg. The patient was sent to the operating room at 2:40 pm and anesthesia was started. Veno-venous ECMO without heparin was set up from 3:20 pm ~ 3:50 pm through cannulation of the superior vena cava and left femoral vein. SpO2 was 100% under ECMO support and emergency surgery was performed at 4:00 pm.

Right postero-lateral thoracotomy revealed

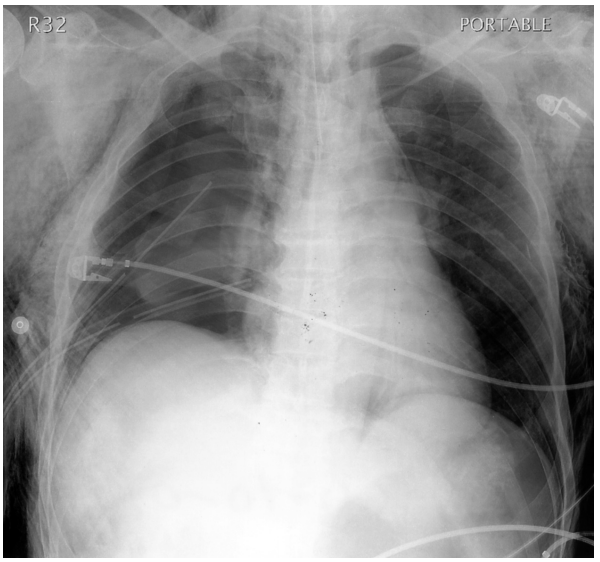

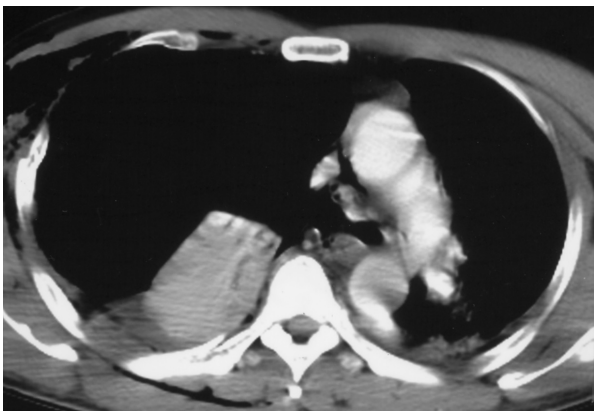

Fig. 1 and 2. Chest X-ray and computed tomography shows pneumothorax, subcutaneous and mediastinal emphysema, and the "fallen lung" sign on the right side.

a 3 cm longitudinal tear in the membranous portion of the trachea and complete transection of the right main bronchus with a free view into the pleural space (Figures 3 and 4). Repair of the tracheal laceration and end-to-end anastomosis of the right main bronchus were performed with interrupted 4-0 PDS II suture. Improved vital signs and full lung expansion 2 days post-operatively enabled the removal of ECMO.

The chest tubes were removed on post-operative days 6 and 10, respectively. For the sake of slowly weaning the patient, his extubation

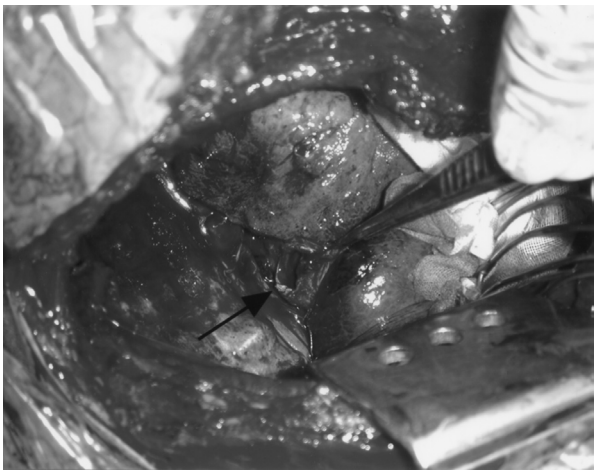

Fig. 3. Right thoracotomy revealed complete transection of the right main stem bronchus (arrow) with a free view into the pleural space.

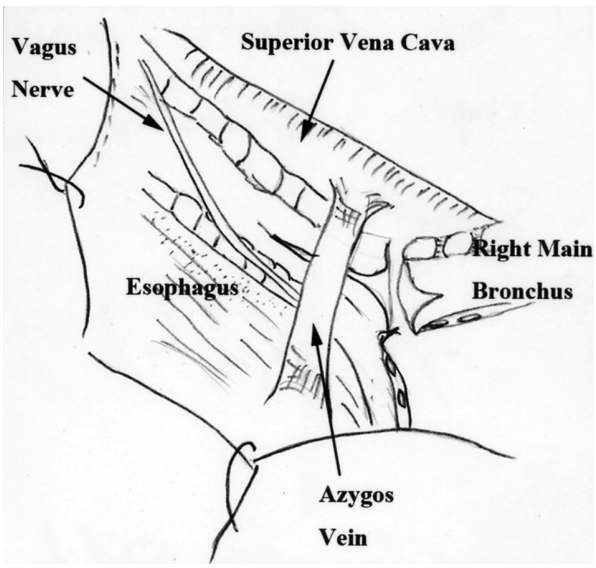

Fig. 4. Schematic illustration of a 3-cm longitudinal tear in the membranous portion of the trachea and complete transection of the right main stem bronchus.

was performed on post-operative day 15. He was sent to the general ward on post-operative day 20 under stable conditions. After orthopedic consultation for his clavicle fracture in this accident, he was transferred to the orthopedics ward for further surgical intervention. Post-operative bronchoscopic examination showed good healing with no stricture. The patient was asymptomatic 18 months after surgery and had a forced vital capacity of 3.13L and forced expiratory volume in 1 minute of 2.2L.

Discussion

Simultaneous tracheal tear and right main bronchus disruption is a highly unusual and life-threatening situation. Possible mechanisms of injury include rapid deceleration with a forward swing of the trachea, widening of the transverse diameter of the chest, traction on the carina, and a rapid rise of airway pressure on impact. Immediate surgical intervention is recommended to avoid loss of lung tissue [2]. Compromised airway, tension pneumothorax, and damage to other vital organs are factors that cause quick death [1]. In blunt trauma, most of the injuries occur within 1 inch of the carina. Major findings on chest radiographs of patients with tracheo-bronchial transection include pneumothorax or pneumo-mediastinum, a “fallen lung” sign, and endotracheal tube abnormalities.

Early bronchoscopic assessment, careful anesthetic management, and meticulous surgical techniques are crucial for a successful outcome. Common complications in the early phase are hypoxia and multiple organ failure, while sepsis, tracheal or bronchial stenosis, mediastinitis, and chronic broncho-pleural fistula are noted in the late phase [3]. Bronchoscopy and chest CT can confirm the diagnosis. In addition, bronchoscopy-guided intubation of the contralateral main bronchus may be necessary to provide adequate ventilation and prevent further tension pneumothorax.

In the current case, veno-venous ECMO support, aside from the ventilator, was used to improve the poor saturation of single-lung ventilation. ECMO is performed in many trau-

matic lung injury and pediatric tracheal stenosis patients to provide oxygen supplementation in reconstruction [4]. Good survival and outcomes are noted in the medical literature. Systemic tissue oxygenation and cardio-pulmonary support can be maintained during the peri- and post-operative period via the extra-corporeal circuit, to minimize lung barotrauma from prolonged high positive pressure. This requires lower amounts of heparin and reduces the risk of hemorrhage as compared to traditional cardio-pulmonary bypass. It is a good alterative for trauma patients with an unstable hemodynamic status.

While conservative treatment for localized short laceration, using antibiotics and intubation with the cuff inflated distal to the tear, is favored by some authors, surgical repair is unavoidable in many cases that involve the whole thickness of the tracheal wall [5]. Even if tracheo-bronchial injury can be managed by primary closure, the length and location of the lesion, degree of pneumothorax or pneumo-mediastinum, and clinical signs are often considered in decision-making, especially for surgery. Thoracotomy is indicated in tracheal lacerations extending to the main bronchi because of its efficacy in reaching and suturing lesions extending to the carina.

In conclusion, early detection and treatment of bronchial transection are important. ECMO can be successfully used in these patients for adequate oxygen supplementation and tissue perfusion before and after surgery.

References

1. Bertelsen S, Howitz P. Injuries of the trachea and bronchi. Thorax 1972; 27: 188-94.
2. de la Rocha AG, Kayler D. Traumatic rupture of the tracheobronchial tree. Can J Surg 1985; 28: 68-71.
3. Glinjongol C, Pakdirat B. Management of tracheo-bronchial injuries: a 10-year experience at Ratchaburi hospital. J Med Assoc Thai 2005; 88: 32-40.
4. Cordell-Smith JA, Roberts N, Peek GJ, *et al*. Traumatic lung injury treated by extra-corporeal membrane oxygenation (ECMO). Injury 2006; 37: 29-32.
5. Gabor S, Renner H, Pinter H, *et al*. Indications for surgery in tracheo-bronchial ruptures. Eur J Cardiothorac Surg 2001; 20: 399-404.

在葉克膜支持下創傷性氣管完全分離的成功修補：病例報告

梁嘉儀　黃培銘　柯文哲*　李元麒

胸部挫傷而造成的氣管完全分離的病例是不常見但致死率高，大約80%以上的病人在事發現場已死亡。因此，救援過程中心肺的維持與足夠氧氣的提供對此類病人的生存率是十分重要。本病例是一個47歲男性，在工作時被重型機器壓倒。於急診處，病人呼吸急促，右側大量氣胸並置入胸管。支氣管鏡顯示右側主氣管斷裂故進行氣管插管並進行單肺呼吸。由於病人血氧分壓沒能有效維持，在手術前放置了葉克膜以提供足夠的氧氣及穩定心肺的功能。病人利用右側開胸手術以進行氣管縫合，術後病人復原情況理想，術後兩天移除葉克膜。現病人在門診持續追蹤，沒有明顯的呼吸困難，肺功能也在正常值內。葉克膜多應用在創傷性肺部，以減少因正壓呼吸而引起的傷害以及兒童氣管狹窄重建手術，不管在術中或術後都可提供全身組織的氧氣及心肺的支持。*(胸腔醫學 **2010; 25: 263-267**)*

關鍵詞：支氣管分離，葉克膜

台大醫院　外科部　胸腔外科，*創傷醫學部
索取抽印本請聯絡：李元麒醫師，國立台灣大學附設醫院　胸腔外科，100台北市中山南路七號

Systemic Air Embolism Following Computed Tomography-Guided Transthoracic Needle Biopsy – A Case Report

Hui-Yuan Hsiao*, Yao-Min Ting*,****, Ming-Wei Weng**, Ming-Ting Wu***,****, Ruay-Sheng Lai *,****

Percutaneous transthoracic needle biopsy is a common procedure for diagnosing pulmonary and mediastinal lesions. The procedure has many potential complications, ranging from simple pneumothorax or self-limiting hemoptysis to life-threatening pulmonary hemorrhage and air embolism [1]. Introducing gas into the circulation is a major iatrogenic problem which could result in serious morbidity and even death. Among the complications of percutaneous transthoracic needle biopsy, systemic air embolism is life-threatening but extremely rare, with an incidence rate of 0.02% to 0.4%. We reported a case of massive systemic air embolism following computed tomography-guided needle biopsy of a pulmonary lesion. After initial resuscitation, the patient received on-site hyperbaric oxygen therapy and demonstrated no residual clinical sequelae from this complication. Pulmonologists should be aware of this rare complication of systemic air embolism. Prompt recognition and immediate hyperbaric oxygen therapy after initial supportive measures are essential to improve the odds of clinical recovery. ***(Thorac Med 2010; 25: 268-274)***

Key words: air embolism, CT-guided biopsy, hyperbaric oxygen therapy

Introduction

Computed tomography (CT)-guided needle biopsy of the lung is a common diagnostic procedure for pulmonary and mediastinal lesions. The most frequent complication is pneumothorax, followed by pulmonary hemorrhage and hemoptysis [1]. Air embolism is an extremely rare but potentially fatal complication [1-4]. In this report, we describe the case of 68-year-old man with several left upper lobe nodules. A CT-guided needle biopsy of the largest pulmonary nodule was undertaken, but was complicated by systemic air embolism. We administered immediate resuscitative measures and subsequent hyperbaric oxygen (HBO) therapy, which resulted in a full recovery without any residual sequelae from this uncommon complication.

*Division of Chest Medicine, Department of Internal Medicine, Kaohsiung Veterans General Hospital, Kaohsiung, Taiwan; **Department of Internal Medicine, Zuoying Armed Forces General Hospital, Kaohsiung, Taiwan; ***Department of Radiology, Kaohsiung Veterans General Hospital, Kaohsiung, Taiwan; ****National Yang-Ming University School of Medicine, Taipei, Taiwan
Address reprint requests to: Dr. Yao-Min Ting, Division of Chest Medicine, Department of Internal Medicine, Kaohsiung Veterans General Hospital, 386, Ta-Chung 1st Road, Kaohsiung 813, Taiwan

Case Report

A 68-year-old man was admitted to our hospital for evaluation of multiple nodules in the left upper lobe on a conventional chest radiograph taken as part of an annual health check-up (Figure 1). A chest CT scan showed a lobulated mass, 3.3×2.2×2 cm in size, in the peripheral region of the left upper lobe, with 2 satellite nodules of 2.2 cm and 1 cm, each, at the peripheral zone. Although the patient had a history of heavy smoking, his serum tumor markers, such as squamous cell carcinoma-related antigen, neuron-specific enolase, and carcinoembryonic antigen, were nevertheless not elevated. Although the findings were not suggestive of malignancy, CT-guided biopsy was requested to establish the diagnosis.

The patient was placed in the prone position and the largest pulmonary nodule was localized using CT. Under CT-fluoroscopy guidance with a step-and-shoot approach, a 19-gauge, 13-cm TruGuid coaxial biopsy needle (Sure Cut®, Temno, Japan) was placed in the larger lesion on the first pass during a single inspiratory breath-holding (Figure 2A). Biopsies were performed using a spring-loaded biopsy gun with a 21-gauge, 16-cm core tissue biopsy needle (Jamshidi-Menghini®, Temno, Japan). This introducer needle was not moved until the end of the procedure, and scans obtained at intervals during the procedure showed its position to be unchanged relative to the pulmonary mass. The coaxial needle was occluded either by an internal blunt-tip stylet or, during sampling, by the radiologist's finger. This ensured that the needle was open to the atmosphere for only very short periods.

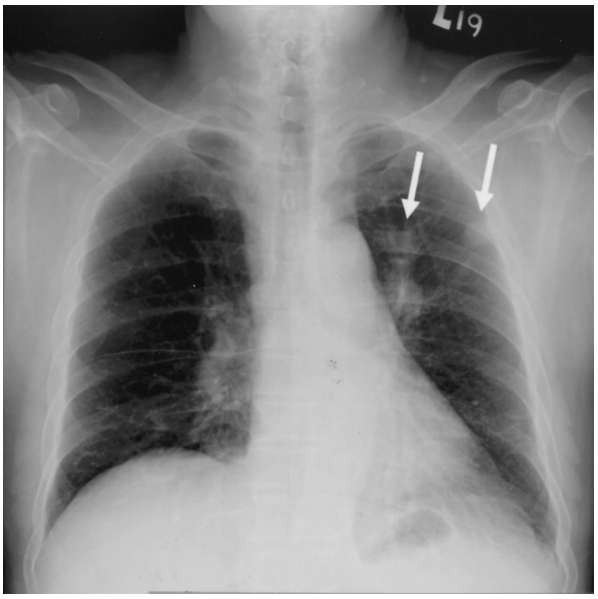

Fig. 1. Anteroposterior chest X-ray showing flattening of bilateral hemidiaphragms with a relatively normal-sized heart and multiple nodules (arrow) in the left upper lobe.

The patient was entirely cooperative and did not cough during the procedure. After the procedure, 3 aspirated biopsy specimens had been collected. The patient was asymptomatic with stable cardiac and respiratory monitoring parameters. However, the follow-up post-procedural CT scan images revealed systemic free air in the descending aorta (Figure 2B). He was then placed in the Trendelenburg position immediately and instructed not to change the position; 100% oxygen was offered immediately through a non-rebreathing mask, and cardiac and respiratory parameters were closely monitored. Initial vital signs remained stable while the oxygen saturation reached 98%.

The patient was transferred to an HBO chamber within 60 minutes of the event, and received 100% oxygen at a pressure of 2.5 atmospheres absolute for 60 minutes. After the treatment, he remained asymptomatic. The chest and brain CT scan images obtained 3 hours later revealed resorption of the preexisting systemic air and no cerebral air, respectively (Figure 3). In addition, the brain CT scan showed unexpected

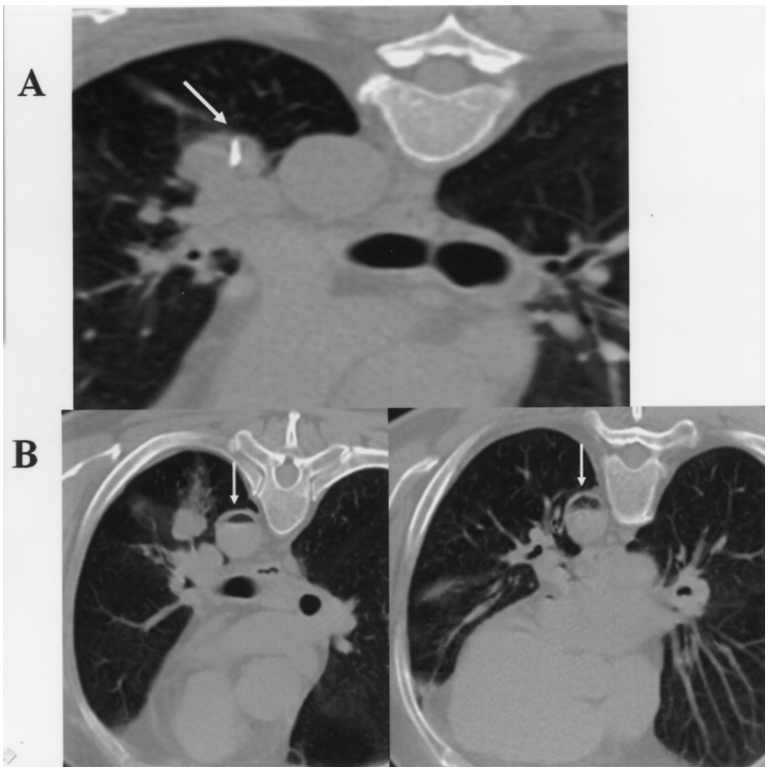

Fig. 2. Top, A: CT fluoroscopic image obtained during the biopsy procedure with the patient in the prone position shows that the internal stylet of a biopsy needle (arrow) was introduced into a tumor in the lung. The arrowhead indicates the tip of an introducer needle. Bottom, B: post-procedural CT scan image with the patient in the prone position shows a small amount of air (arrow) in the descending aorta. Post-biopsy hemorrhage was noted around the path of the biopsy needle.

metastasis with the presence of several enhancing nodular lesions in the parenchyma. The histologic examination of the biopsy specimens demonstrated small cell carcinoma.

Discussion

Percutaneous transthoracic lung biopsy is a relatively common procedure with considerable importance in the management of patients. As these invasive procedures become more common, the occurrence of complications becomes more of a problem. The published complication rates vary widely. Pneumothorax is reported as the most frequent complication, with an incidence rate of 20.5-49%. Intraparenchymal hemorrhage and hemoptysis, occurring in about 11% and 5.3-7% of cases, respectively, have become the second and third most frequently seen complications [1-2]. Systemic air embolism is recognized as an extremely rare complication of transthoracic needle biopsy. To our knowledge, only 19 cases of air embolism after percutaneous needle biopsy of the lung have been reported in the English literature [5-9], and the incidence has varied from 0.02% in a United Kingdom study to 0.4% in a Japanese study [1-4]. Extensive CT scanning after the procedure and the considerable attention that has been focused on systemic air embolism might explain

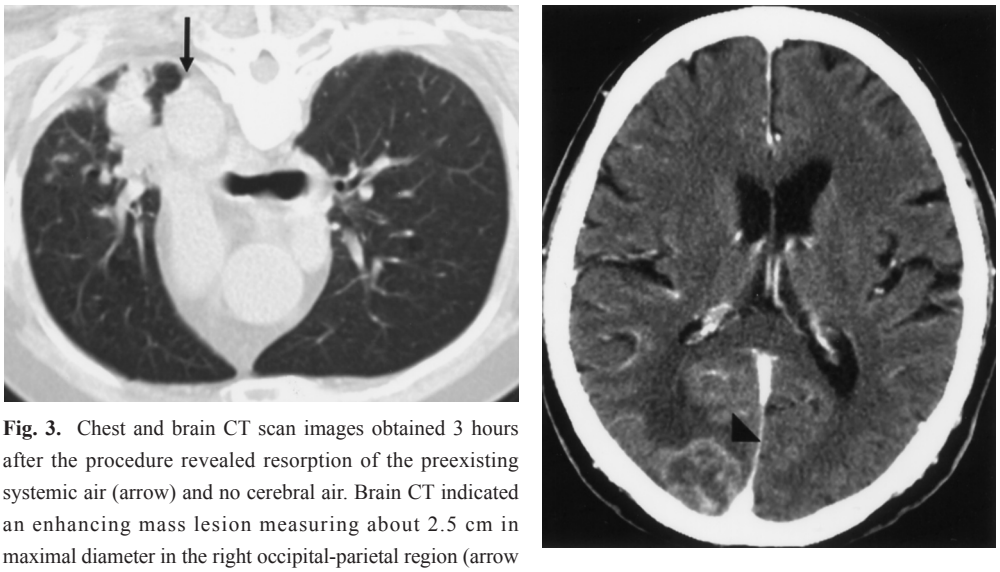

Fig. 3. Chest and brain CT scan images obtained 3 hours after the procedure revealed resorption of the preexisting systemic air (arrow) and no cerebral air. Brain CT indicated an enhancing mass lesion measuring about 2.5 cm in maximal diameter in the right occipital-parietal region (arrow head), with marked perifocal edema and a mass effect causing compression of the occipital horn of the right lateral ventricle, compatible with brain metastasis.

this increasing trend in the incidence.

In the reports mentioned above, most cases of systemic air embolism resulted in cerebral and/or cardiac morbidity, which often caused death. Tomiyama *et al*. described a case of asymptomatic systemic air embolism in which the embolism occurred regardless of the location of the lesion, needle size, procedural positioning, or sampling method (aspiration or cutting); the following contributing factors were considered: positive-pressure ventilation, coughing during the procedure, the needle tip was placed within the pulmonary vein, and the procedure was performed for a cavitary or cystic lesion and in a patient with necrotizing vasculitis [3]. The prompt diagnosis of systemic air embolism depends largely on routinely performed post-procedural scanning of the entire thorax, rather than the clinical manifestation of a rapid deterioration of neurologic and/or cardiac status.

There are several mechanisms that lead to systemic air embolism [10]. First, when the needle tip is placed within the pulmonary vein, the vein comes into contact with the atmosphere after the removal of the internal stylet. When the atmospheric pressure exceeds the venous pressure, for example, during inspiration, air may be introduced into the vein. Second, when the needle traverses the pulmonary vein and the airway at the same time, a bronchovenous fistula forms. Positive-pressure ventilation, the Valsalva maneuver, and most importantly, coughing increase airway pressure. The risk of systemic air embolism may be increased when airway pressure is elevated. Third, during vascular injury, the walls of small vessels adhere spontaneously and become sealed, or muscular vessels may retract. Extravasated and then coagulated blood may promote extravascular tamponade. However, coagulopathy or vasculitis may interfere with this healing process, resulting in prolonged exposure of the vessel lumen to the airway.

The primary treatment for systemic air em-

bolism involves supplying 100% oxygen, which may promote the replacement of the nitrogen within the air with oxygen, thereby facilitating the resorption of the air. There are some controversies regarding the positioning of the patient with systemic air embolism. Baker *et al*. and MacLean recommended the application of left lateral decubitus and Trendelenburg positioning if the air bubble is detected in the left ventricle before embolizing to the brain. Placing the patient in such a position appears to reduce the risk of cerebral embolism by keeping the air away from the ventricular outflow tracts [5, 11]. On the other hand, other investigators are of the opinion that the buoyancy of gas bubbles is not sufficient to counteract the blood flow; they recommend the use of the flat supine position [12].

The mainstay treatment is HBO therapy. The volume of gas in an enclosed space is inversely proportional to the pressure exerted on it. In addition, this therapy accelerates the dissolution of nitrogen by replacing the nitrogen with oxygen, which is subsequently metabolized at a rapid rate by the tissue [13]. The strategy of HBO therapy for symptomatic subjects varies among different medical associations. Grant *et al*. reported the case of a patient with massive systemic air embolism complicating percutaneous transthoracic needle biopsy who received 3 dives of HBO therapy (100% oxygen at the pressure of 6 atmospheres absolute for 25 minutes), resulting in complete recovery to his preprocedural clinical baseline level of functioning [8]. Recently, Um *et al*. commenced HBO therapy in 3 cases of cerebral air embolism following percutaneous transthoracic needle biopsy, 2 of the patients received 100% oxygen at a pressure of 2.2 atmospheres absolute for 110 minutes and the other for 60 minutes. All 3 patients recovered fully without any neurologic sequelae [14]. However, optimal treatment strategies for asymptomatic cases of systemic air embolism remain to be determined. Hiraki *et al*. reported 4 cases of non-fatal systemic air embolism after a percutaneous transthoracic needle biopsy. HBO therapy was performed for 2 of them, at a pressure of 3.1 atmospheres absolute for 120 minutes, and resorption of preexisting air developed without any clinical sequelae. The other 2 patients were treated conservatively with 100% oxygen; 1 fully recovered and the other presented with acute cerebral infarction resulting in a permanent neurologic deficit [4]. According to these reports, the institution of HBO therapy with a lower atmosphere and prolonged duration may constitute curative treatment. We also used this principle in the treatment of our case: HBO therapy with 100% oxygen was offered at a pressure of 2.5 atmospheres absolute for 60 minutes. In any case, successful treatment largely depends on the early recognition of this event and the prompt application of the therapy.

A number of preventive measures would effectively minimize the risk and the morbidity of the intervention as well. As far as possible, the needle path should avoid pulmonary vessels and bronchi. The needle should be exposed to the atmosphere for as short a time as possible, and the patient should be instructed to suspend respiration at that time to potentially prevent air from being introduced into the vascular system. The opening should be closed immediately with either a physician's finger or by the introduction of a biopsy needle. Puncture of lesions communicating with the airways might promote coughing or hemoptysis, thereby creating a favorable pressure gradient for air embolism. Keeping the patient from coughing would minimize the potential for introducing air. For the same reason, positive-pressure ventilation is considered as a

contraindication for needle biopsy. However, it should be remembered that this complication can occur even when excellent techniques are applied to a cooperative patient by an experienced, skillful physician. In our case, all of the risk factors and preventive maneuvers mentioned above had been noted. The probable cause of the formation of systemic air embolism could have been the centrally located nodule we found and approached.

Pulmonologists who refer patients to the radiology department should be aware of this rare complication following percutaneous transthoracic biopsies of pulmonary lesions, and fully explain the possible risks to the patients before invasive procedures are scheduled to be performed at all times. As demonstrated in this case, prompt recognition and immediate HBO therapy after initial supportive measures are essential to improve the odds of clinical recovery.

References

1. Sinner WN. Complications of percutaneous transthoracic needle aspiration biopsy. Acta Radiol Diagn (Stockh) 1976; 17: 813-28.
2. Richardson CM, Pointon KS, Manhire AR, *et al*. Percutaneous lung biopsies: a survey of UK practice based on 5444 biopsies. Br J Radiol 2002; 75: 731-5.
3. Tomiyama N, Yasuhara Y, Nakajima Y, *et al*. CT-guided needle biopsy of lung lesions: a survey of severe complication based on 9783 biopsies in Japan. Eur J Radiol 2006; 59: 60-4.
4. Hiraki T, Fujiwara H, Sakurai J, *et al*. Nonfatal systemic air embolism complicating percutaneous CT-guided transthoracic needle biopsy: four cases from a single institution. Chest 2007; 132: 684-90.
5. Baker BK, Awwad EE. Computed tomography of fatal cerebral air embolism following percutaneous aspiration biopsy of the lung. J Comput Assist Tomogr 1988; 12: 1082-3.
6. Kodama F, Ogawa T, Hashimoto M, *et al*. Fatal air embolism as a complication of CT-guided needle biopsy of the lung. J Comput Assist Tomogr 1999; 23: 949-51.
7. Arnold BW, Zwiebel WJ. Percutaneous transthoracic needle biopsy complicated by air embolism. AJR Am J Roentgenol 2002; 178: 1400-2.
8. Lattin G Jr, O'BrienWSr, McCrary B, *et al*. Massive systemic air embolism treated with hyperbaric oxygen therapy following CT-guided transthoracic needle biopsy of a pulmonary nodule. J Vasc Interv Radiol 2006; 17: 1355-8.
9. Hirasawa S, Hirasawa H, Taketomi-Takahashi A, *et al*. Air embolism detected during computed tomography fluoroscopically guided transthoracic needle biopsy. Cardiovasc Interv Radiol 2008; 31: 219-21.
10. Kau T, Rabitsch E, Celedin S, *et al*. When coughing can cause stroke--a case-based update on cerebral air embolism complicating biopsy of the lung. Cardiovasc Intervent Radiol 2008; 31: 848-53.
11. MacLean CA, Bachman DT. Documented arterial gas embolism after spinal epidural injection. Ann Emerg Med 2001; 38: 592-5.
12. Muth CM, Shank ES. Gas embolism. N Engl J Med 2000; 342: 476-82.
13. Tibbles PM, Edelsberg JS. Hyperbaric-oxygen therapy. N Engl J Med 1996; 334: 1642-8.
14. Um SJ, Lee SK, Yang DK, *et al*. Four cases of a cerebral air embolism complicating a percutaneous transthoracic needle biopsy. Korean J Radiol 2009; 10: 81-4.

電腦斷層導引肺部細針切片引起之全身性空氣栓塞症：一病例報告

蕭惠元* 丁燿明*,**** 翁銘偉** 吳銘庭***,**** 賴瑞生*,****

經皮細針胸腔穿刺切片經常用來診斷肺部及縱膈腔疾病，這項檢查可能造成一些併發症，諸如：單純性氣胸、自限性咳血、致命性肺出血及空氣栓塞症。將空氣導入心血管循環系統是一個危險的醫源性傷害，可造成嚴重病症甚至死亡，在所有經皮細針胸腔穿刺切片檢查中，它的發生率介於0.02%到0.4%間。在此我們報告一位患者接受電腦斷層導引切片後，經電腦斷層證實，併發大量全身性空氣栓塞症，初步給予氧氣並穩定生命徵象後，患者接受立即的高壓氧治療，追蹤後並無發生空氣栓塞症相關的後遺症。對於全身性空氣栓塞這個少見的併發症，胸腔醫師必須熟悉且注意，能夠及時診斷並給予高壓氧治療。*(胸腔醫學* ***2010; 25: 268-274)***

關鍵詞：空氣栓塞症，電腦斷層導引切片，高壓氧

*高雄榮民總醫院 胸腔內科，**國軍左營總醫院 內科部，***高雄榮民總醫院 放射科，****國立陽明大學醫學院
索取抽印本請聯絡：丁燿明醫師，高雄榮民總醫院內科部 胸腔內科，高雄市左營區大中一路386號

Thoracoscopic Diagnosis of Right-sided Bochdalek Hernia in an Adult with Traumatic Injury

Yin-Chun Chang*, Chin-Chih Chang*,**, Wen-Je Ko*,**, Yung-Chie Lee*

A 49-year-old woman was injured in a motor vehicle accident. Rupture of the right diaphragm and liver herniation were suspected from the chest radiography and computed tomographic scan. However, due to the lack of a definite diagnosis, a diagnostic thoracoscopy was performed which revealed a right-sided Bochdalek hernia with partial liver herniation. A normally developed liver and no herniation of the abdominal viscera were also noted. The patient had an uneventful recovery after the operation and maintained regular follow-up after discharge. Right-sided Bochdalek hernia in an adult could be mimicked by traumatic diaphragm rupture. The diagnosis can be confirmed by means of minimally invasive thoracoscopy which is a good diagnostic tool. ***(Thorac Med 2010; 25: 275-278)***

Key words: Bochdalek hernia, diaphragm rupture, thoracoscopy

Case Report

A 49-year-old woman was admitted to the emergency department after a motor vehicle accident. She had been hit laterally on her left side by a car while she was riding a motorcycle. The patient complained of severe headache and lower back pain with lower limb numbness. Physical examination was unremarkable and the Glasgow coma scale was E4M6V5. Blood studies revealed a white blood cell count of 7.19 K/μL, a hemoglobin level of 12.9 g/dL, and an aspartate aminotransferase level of 29 U/l. A plain radiography revealed T12 and L1 spinal fracture, and chest plain radiography revealed faint patchy opacities in the right diaphragm (Figure 1). Chest and abdomen computed tomographic (CT) scans showed a suspicious right posterior diaphragmatic rupture with hernia of the posterior superior lobe of the liver (Figure 2a). The reformatted sagittal view of the CT scan revealed a dumbbell-shaped liver with a bulging portion above the diaphragm (Figure 2b). However, with no definite diagnosis after the imaging study, a diagnostic thoracoscopy was performed which revealed a right posterolateral diaphragm defect with partial liver herniation. The liver surface was smooth, without laceration and bleeding, and no other abdominal viscera herniation in the thoracic cavity was noted (Figure 3). A congenital right-sided Bochdalek hernia with partial liver herniation

Department of Surgery* and Traumatology**, National Taiwan University Hospital and National Taiwan University College of Medicine, Taipei, Taiwan
Address reprint requests to: Dr. Yung-Chie Lee, Division of Thoracic Surgery, Department of Surgery, National Taiwan University Hospital, 7, Chung-Shan S. Rd, Taipei 100, Taiwan

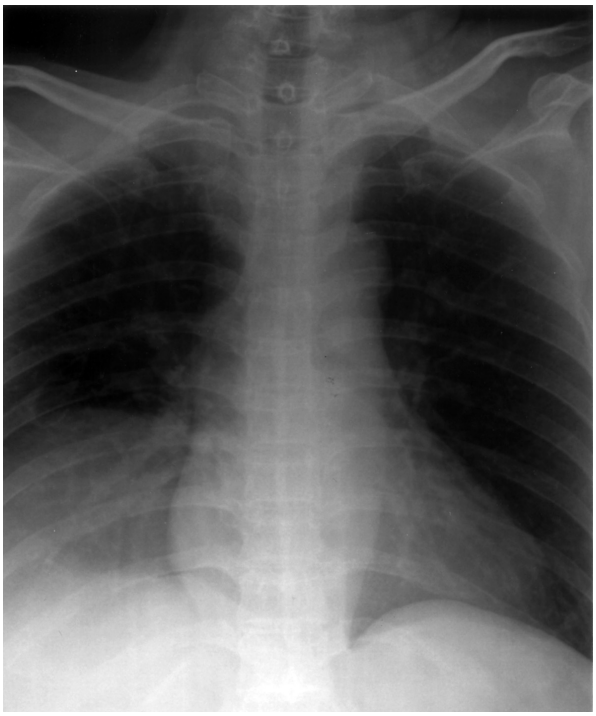

Fig. 1. Chest radiography showing faint patchy opacities in the right diaphragm

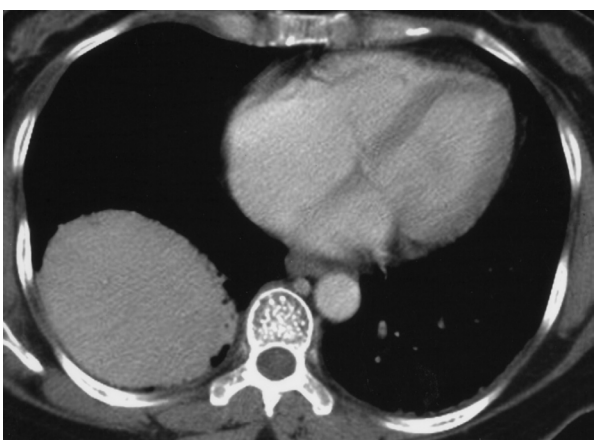

Fig. 2a. Chest CT scan showing a suspicious right posterior diaphragmatic rupture with hernia of the posterior superior lobe of the liver

was confirmed. No further diaphragm repair was performed because of the tight adhesion of the diaphragm edge and liver. The patient had an uneventful recovery after the operation and maintained regular follow-up after discharge.

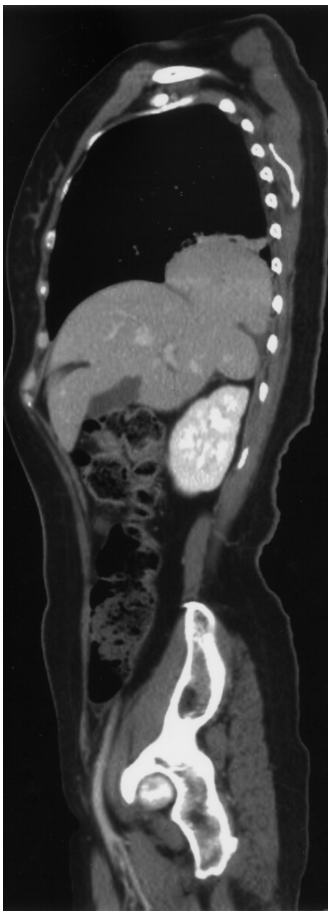

Fig. 2b. Chest reformatted sagittal view revealing a dumbbell-shaped liver with a bulging portion above the diaphragm

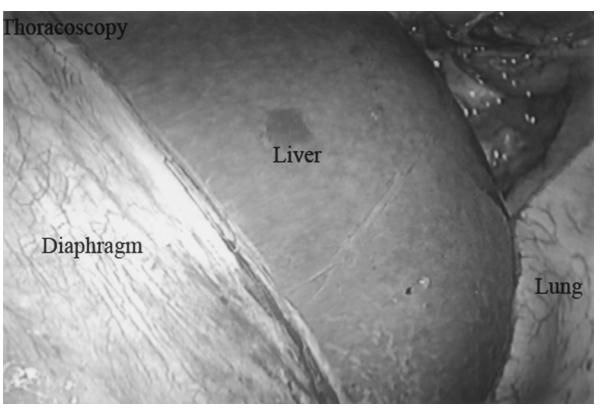

Fig. 3. Thoracoscopy showing a Bochdalek hernia with liver herniation

Discussion

In 1848, Bochdalek first described the congenital, improper fusion of the posterolateral foramina of the diaphragm, now called a Bochdalek hernia. This type of hernia is more commonly diagnosed in children, with a presentation of respiratory insufficiency, and is rarely diagnosed in adults. Gale *et al*. found that the incidence of adult Bochdalek hernia was 6%, and only 35% were right-sided [1]. Right-sided Bochdalek hernias are even rarer because the herniation of the intra-abdominal viscera to the plural cavity is prevented by the liver. Traumatic diaphragm rupture (TDR) is relatively rare. The incidence rates of TDR caused by blunt trauma are between 0.8 and 1.6%. Left-sided rupture is more common than right-sided rupture, which may be due to protection by the liver and the increased strength of the right hemidiaphragm [2].

Bochdalek hernia may be found incidentally in asymptomatic adults when investigating for other diseases, but sometimes this condition may be confused with TDR in trauma patients. Multiple imaging modalities are available for the evaluation of diaphragm defects. The reported sensitivity of chest radiography is 17% for right-sided TDR, and the sensitivity of abdominothoracic CT scans for diagnosis of TDR is 33% to 83% [3]. Magnetic resonance imaging (MRI) for diagnosis of TDR has been used in only a few case reports [4]. Thoracoscopic examination should be considered in cases where imaging is not conclusive. This procedure is minimally invasive, and can be used to evaluate diaphragm defects, including damage to other organs, under direct vision. Furthermore, surgical intervention can be performed at the same time.

Making an early diagnosis of TDR in trauma patients is challenging for physicians. We present this case to emphasize the usefulness of diagnostic thoracoscopy as an effective tool for evaluating patients with suspected diaphragm injury.

References

1. Gale ME. Bochdalek hernia: prevalence and CT characteristics. Radiology 1985; 156(2): 449-52.
2. Lee WJ, Lee YS. Traumatic diaphragmatic rupture: a diagnostic challenge in the emergency department. Emerg Med J 2007; 24(8): 601.
3. Sato M, Kosaka S. Minimally invasive diagnosis and treatment of traumatic rupture of the right hemidiaphragm with liver herniation. Jpn J Thorac Cardiovasc Surg 2002; 50(12): 515-7.
4. Boulanger BR, Mirvis SE, Rodriguez A. Magnetic resonance imaging in traumatic diaphragmatic rupture: case reports. J Trauma 1992; 32(1): 89-93.

胸腔鏡診斷右側橫膈疝氣疑似創傷性橫膈破裂——病例報告

張彥俊* 張金池*,** 柯文哲*,** 李元麒*

49歲女性病患，因車禍而來急診就診。胸部X光影像及胸部電腦斷層影像疑似橫膈破裂及肝疝氣。因無法確定診斷，病人接受了診斷性胸腔鏡手術。手術發現右側橫膈Bochdalek疝氣及部分肝臟疝氣，沒有發現其他腹部器官疝氣。術後病人恢復良好，目前持續追蹤中。成人右側橫膈Bochdalek疝氣疑似創傷性橫膈疝氣由微創性胸腔鏡是很好的診斷工具。*(胸腔醫學* ***2010; 25: 275-278)***

關鍵詞：橫膈Bochdalek疝氣，橫膈破裂，胸腔鏡

國立台灣大學醫學院附設醫院 外科部*，創傷醫學部**
索取抽印本請聯絡：李元麒醫師，國立台灣大學醫學院附設醫院 外科部，台北市中山南路7號

Prostate Cancer with Mediastinal Lymph Node Metastasis Diagnosed by Transbronchial Needle Aspiration: A Case Report

Kuei-Pin Chung, Chao-Chi Ho, Chong-Jen Yu

Prostate cancer metastases usually involve the skeletal system or regional lymph nodes. Mediastinal lymph node metastases are rare in prostate cancer, and may develop at presentation or during treatment. Before the introduction of endobronchial ultrasonography, invasive procedures such as mediastinoscopy or thoracoscopy were required for the definite diagnosis. With the application of convex probe endobronchial ultrasonography-guided transbronchial needle aspiration (EBUS-TBNA), the etiology of mediastinal lymphadenopathy can be confirmed and more invasive methods avoided. We described a 67-year-old man with prostate cancer who subsequently developed mediastinal lymph node metastases and pulmonary lymphangitis carcinomatosis during the treatment course. The diagnosis of mediastinal lymph node metastases was confirmed by EBUS-TBNA. We concluded that mediastinal lymph node metastases could develop in prostate cancer and could be confirmed by EBUS-TBNA. ***(Thorac Med 2010; 25: 279-285)***

Key words: prostate cancer, mediastinal lymphadenopathy, endobronchial ultrasonography, transbronchial needle aspiration

Introduction

Mediastinal lymphadenopathy is most often caused by lymphoma, metastatic cancer, and granulomatous disease. The origins of mediastinal lymph node metastases include head and neck cancer, breast cancer, lung cancer, genitourinary cancer, and melanoma [1-2]. Mediastinal lymphadenopathy is relatively rarely the result of metastases from malignancies below the diaphragm. Metastases from prostate cancer usually involve the axial skeleton, appendicular bones, and regional lymph nodes. Mediastinal lymph node metastases due to prostate cancer are unusual, and may occur alone or in combination with pulmonary metastases or lymphangitis carcinomatosis [3-4]. Therefore, for patients with prostate cancer and mediastinal lymphadenopathy, a pathological diagnosis is required to exclude other possible diseases, including lymphoma or granulomatous diseases, such as tuberculous lymphadenitis or sarcoido-

Department of Internal Medicine, National Taiwan University Hospital, National Taiwan University College of Medicine, Taipei, Taiwan
Address reprint requests to: Dr. Chao-Chi Ho, Dept. of Internal Medicine, National Taiwan University, No. 7, Chung-Shan S. Rd., 100 Taipei, Taiwan

sis.

Before the introduction of endobronchial ultrasonography-guided transbronchial needle aspiration (EBUS-TBNA), mediastinoscopy, thoracoscopy, or thoracotomy were the main diagnostic tools for mediastinal lymphadenopathy. Several studies have shown that EBUS-TBNA has good diagnostic accuracy for mediastinal tumor and lymphadenopathy [5-7]. For patients with lung cancer and mediastinal lymphadenopathy, the use of EBUS-TBNA may decrease the need for more invasive procedures [7-8]. EBUS-TBNA has been reported to be diagnostic in 88.7% of mediastinal masses without known pulmonary malignancy [9]. In a literature review, no report was found that mentioned the use of EBUS-TBNA in the diagnosis of mediastinal lymph node metastases from prostate cancer. Herein, we report a case with mediastinal lymph node metastases from prostate cancer that was diagnosed by EBUS-TBNA.

Case Report

A 67-year-old man was admitted due to gross hematuria in January 2008. Pelvic computed tomography (CT) showed an enlarged prostate with bladder invasion. Transurethral resection of the bladder tumor and prostate was performed. The pathology showed adenocarcinoma, with prostate-specific antigen (PSA) expression. Prostatic adenocarcinoma with a Gleason score of 8 and clinical stage IV was diagnosed, and the patient was given monthly leuprorelin as hormonal treatment. However,

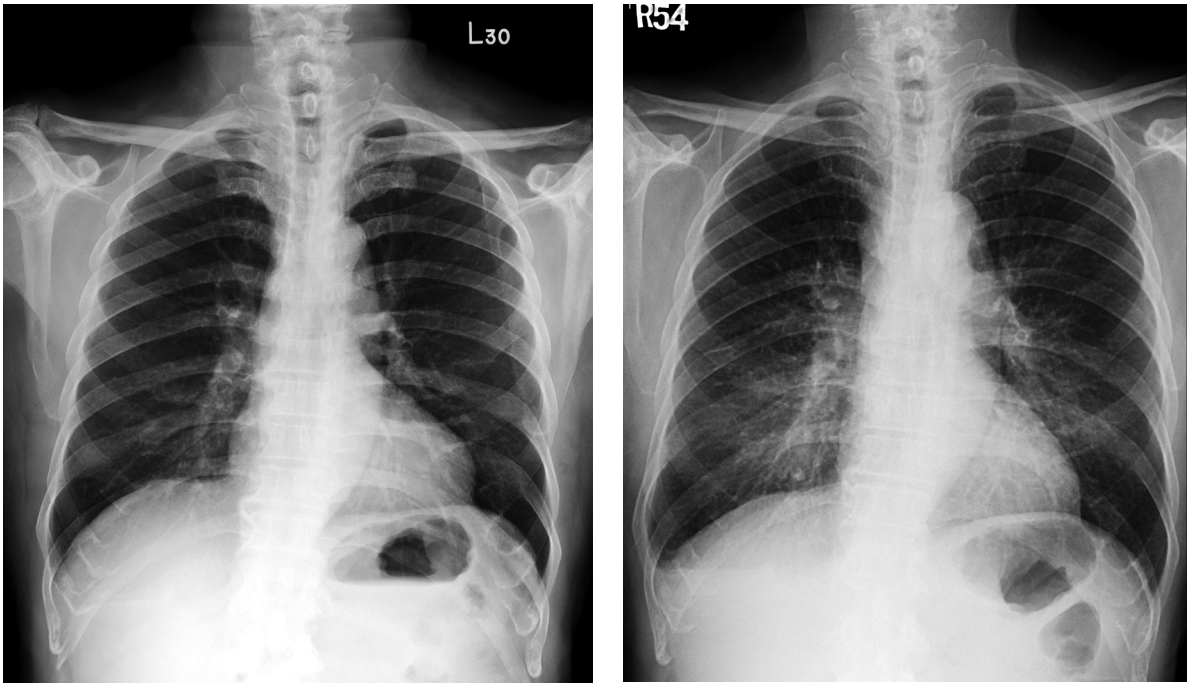

(A) (B)

Fig. 1. Chest radiographs at presentation and during the treatment course. (A) Chest radiograph at presentation did not show enlarged hila or increased parenchymal infiltrations. (B) Chest radiograph during the treatment course showed enlarged hila and diffusely increased interstitial infiltrations in the bilateral lung fields.

the serum PSA level increased gradually from 0.5 ng/mL to 11 ng/mL from February to May 2009. Multiple bony metastases were found by bone scan. Palliative radiotherapy, followed by bicalutamide treatment, was administered. Nevertheless, the serum PSA level continued to increase rapidly, reaching 2967 ng/mL by Nov 2009.

Progressive dyspnea developed beginning Nov 2009, together with non-productive cough and significant body weight loss (10 kg in 1 month). Chest radiography showed enlarged hila and increased pulmonary interstitial infiltrations (Figure 1). Chest CT scan showed enlarged lymph nodes at the paratracheal, subcarinal, and hilar zones, together with a thick-

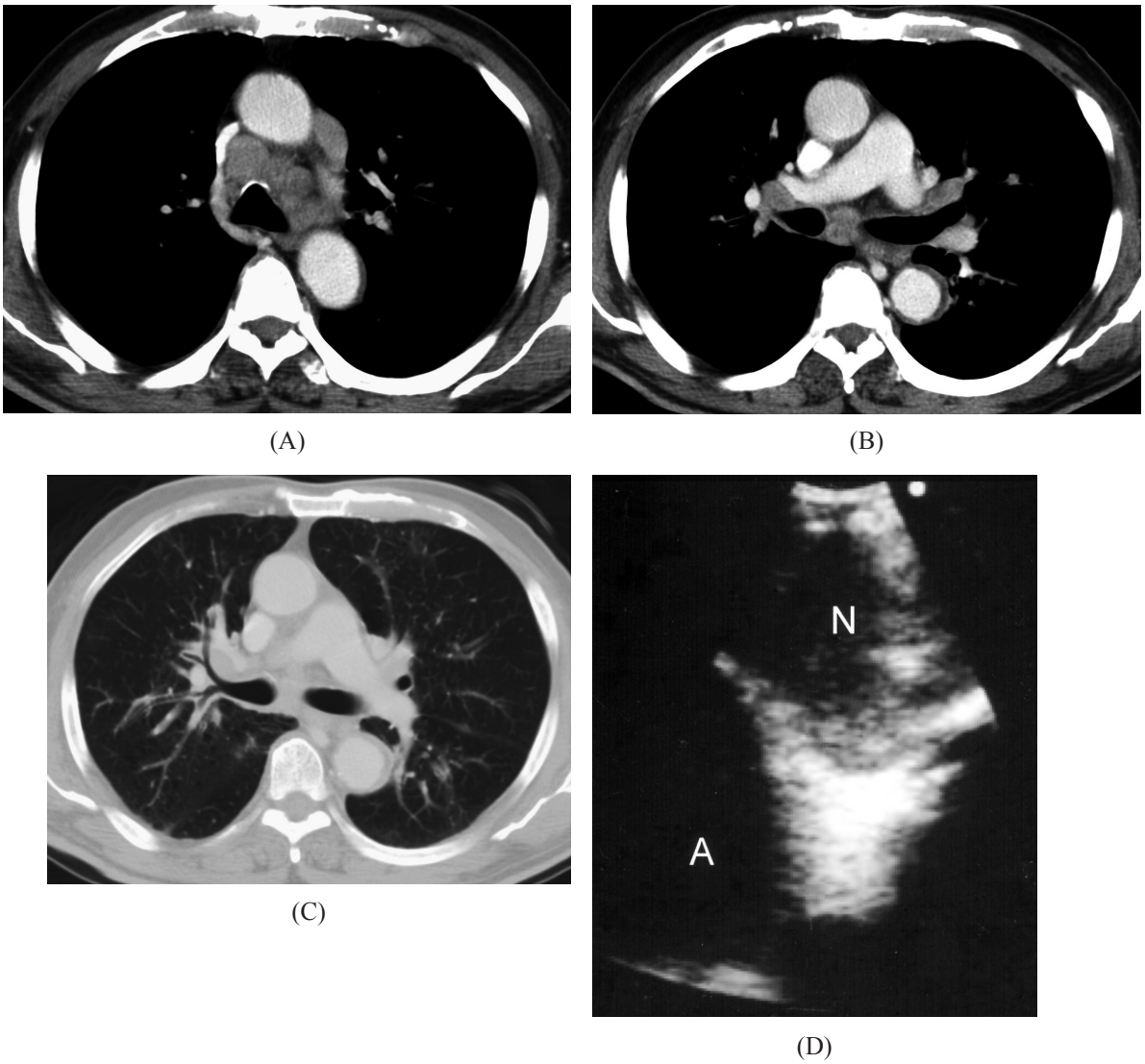

(A) (B) (C) (D)

Fig. 2. Chest computed tomography scan with contrast enhancement. (A) and (B) Prominent mediastinal lymphadenopathies were noted at para-tracheal, subcarinal, and bilateral hilar regions. (C) Thickened peri-bronchovascular interstitium was also found, extending from the bilateral hila. (D) Right lower paratracheal lymph nodes were detected by EBUS. The histologic core was obtained with TBNA. (N: lymph node; A: aorta)

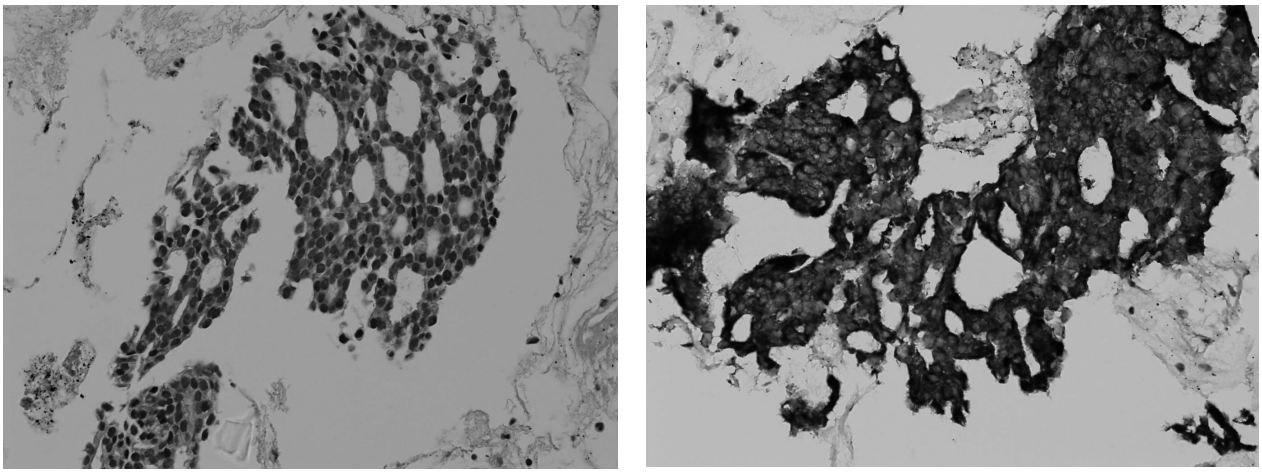

(A) (B)

Fig. 3. Pathologic exam of the histologic core. (A) In the microscopic view, adenocarcinoma cells with a high nuclear-to-cytoplasmic ratio and hyperchromatic nuclei were arranged in solid sheets or a cribriform pattern (400X, H&E stain). (B) Immunohistochemical study showed strong expression of PSA in tumor cells.

ened peri-bronchovascular interstitium (Figures 2A-2C). EBUS-TBNA of the lower paratracheal lymph nodes (zones 4R and 4L) was then performed (Figure 2D). The pathology of the histologic core showed adenocarcinoma. Immunohistochemical study showed negative expression of TTF-1, CK7, and CK-20, but strong expression of PSA in the tumor cells (Figure 3). Prostatic adenocarcinoma with mediastinal lymph node metastases, and probable lymphangitis carcinomatosis, were diagnosed. As of this writing (Mar 2010), the patient has been receiving chemotherapy with docetaxel. The serum PSA level after chemotherapy decreased to 918 ng/mL.

Discussion

Prostate cancer may cause local invasion and pelvic lymph node metastases; the risk of regional lymph node metastases correlates with clinical staging, the biopsy Gleason score, and the serum PSA level [10]. The most common sites of non-regional lymphatic metastases at presentation were the supraclavicular nodes, and only 14% of non-regional lymphatic metastases involved the mediastinal nodes [11]. Mediastinal lymph node metastases can also develop during treatment, but the actual prevalence is unknown. The precise route of lymphatic spread to the mediastinal lymph nodes is not entirely clear. According to a previous report, mediastinal lymph node metastases might occur by extension from the retrocrural and para-aortic nodes into the thoracic duct and its collaterals, followed by retrograde flow from these channels to the mediastinal nodes [2]. For patients with prostate cancer and mediastinal lymph node enlargement, ^{18}F-fluorodeoxyglucose positron emission tomography (PET) does not offer additional information for diagnosis. This is mainly due to the low glucose metabolism in prostate cancer. PET imaging with ^{11}C/^{18}F-choline or ^{11}C/^{18}F-acetate might be useful in evaluating metastases of prostate cancer [12]. However, further study is required to confirm

the clinical role of PET in patients with prostate cancer and mediastinal lymphadenopathy.

Chemokine receptor CCR7 has been associated with lymph node metastases in breast cancer, non-small cell lung cancer, and gastric cancer [13-15]. Indeed, several chemokines and their receptors play important roles in the development of prostate cancer, including tumor growth, angiogenesis, invasion, metastases, and hormone escape [16]. In a previous report, CCR7 expression in tumor epithelium was found in a patient with prostate cancer presenting with generalized lymphadenopathy. It is still unknown if CCR7 expression is related to the pathogenesis of unusual lymph node metastases, as in prostatic cancer. Further studies are needed to clarify the actual role of CCR7 in prostate cancer metastases.

EBUS-TBNA is important in the diagnosis of mediastinal tumors. It is a safe and sensitive tool for nodal staging in lung cancer, and lymph nodes with diameters of 7 mm can also be approached [6, 8]. EBUS-TBNA also has a good diagnostic yield in the evaluation of mediastinal nodes or masses [5-7]. Compared with nodal staging in lung cancer, reaching a definite diagnosis of mediastinal tumors might be difficult due to inadequate specimens for further immunohistochemical studies [9]. PSA and prostatic acid phosphatase were important markers for distinguishing adenocarcinoma of the prostate from others with various origins [4, 17]. In our patient, the histologic core obtained by EBUS-TBNA showed adenocarcinoma with PSA expression, which confirmed prostate cancer with mediastnal lymph node metastases. The more invasive diagnostic procedures, such as mediastinoscopy, were thus avoided. This is the first reported case with both prostate cancer and mediastinal lymph node metastases diagnosed by EBUS-TBNA.

Conclusion

Mediastinal lymph node metastases are unusual in prostate cancer, which might occur together with pulmonary metastases or lymphangitis carcinomatosis. For patients with prostate cancer and mediastinal lymphadenopathy, EBUS-TBNA is a less invasive diagnostic tool for evaluation and to establish the diagnosis of mediastinal lymph node metastases.

Acknowledgments

Potential conflicts of interest. All authors: no conflicts.

References

1. McLoud TC, Kalisher L, Stark P, *et al*. Intrathoracic lymph node metastases from extrathoracic neoplasms. AJR Am J Roentgenol 1978; 131(3): 403-7.
2. Mahon TG, Libshitz HI. Mediastinal metastases of infradiaphragmatic malignancies. Eur J Radiol 1992; 15(2): 130-4.
3. Lindell MM, Doubleday LC, von Eschenbach AC, *et al*. Mediastinal metastases from prostatic carcinoma. J Urol 1982; 128(2): 331-4.
4. Yam LT, Winkler CF, Janckila AJ, *et al*. Prostatic cancer presenting as metastatic adenocarcinoma of undetermined origin. Immunodiagnosis by prostatic acid phosphatase. Cancer 1983; 51(2): 283-7.
5. Herth FJ, Eberhardt R, Vilmann P, *et al*. Real-time endobronchial ultrasound guided transbronchial needle aspiration for sampling mediastinal lymph nodes. Thorax 2006; 61(9): 795-8.
6. Krasnik M, Vilmann P, Larsen SS, *et al*. Preliminary experience with a new method of endoscopic transbronchial real time ultrasound-guided biopsy for diagnosis of mediastinal and hilar lesions. Thorax 2003; 58(12): 1083-6.
7. Yasufuku K, Chiyo M, Sekine Y, *et al*. Real-time endo-

bronchial ultrasound-guided transbronchial needle aspiration of mediastinal and hilar lymph nodes. Chest 2004; 126(1): 122-8.

8. Yasufuku K, Chiyo M, Koh E, *et al*. Endobronchial ultrasound-guided transbronchial needle aspiration for staging of lung cancer. Lung Cancer 2005; 50(3): 347-54.
9. Yasufuku K, Chiyo M, Yamada Y, *et al*. Utility of endobronchial ultrasound-guided transbronchial needle aspiration in the diagnosis of mediastinal masses in the absence of known pulmonary malignancy. Eur Respir J 2005; 26(Suppl 49): 697s.
10. Briganti A, Blute ML, Eastham JH, *et al*. Pelvic lymph node dissection in prostate cancer. Eur Urol 2009; 55(6): 1251-65.
11. Heresi GA, Wang J, Taichman R, *et al*. Expression of the chemokine receptor CCR7 in prostate cancer presenting with generalized lymphadenopathy: report of a case, review of the literature, and analysis of chemokine receptor expression. Urol Oncol 2005; 23(4): 261-7.
12. Bouchelouche K, Oehr P. Recent developments in urologic oncology: positron emission tomography molecular imaging. Curr Opin Oncol 2008; 20(3): 321-6.
13. Muller A, Homey B, Soto H, *et al*. Involvement of chemokine receptors in breast cancer metastasis. Nature 2001; 410(6824): 50-6.
14. Takanami I. Overexpression of CCR7 mRNA in nonsmall cell lung cancer: correlation with lymph node metastasis. Int J Cancer 2003; 105(2): 186-9.
15. Mashino K, Sadanaga N, Yamaguchi H, *et al*. Expression of chemokine receptor CCR7 is associated with lymph node metastasis of gastric carcinoma. Cancer Res 2002; 62(10): 2937-41.
16. Vindrieux D, Escobar P, Lazennec G. Emerging roles of chemokines in prostate cancer. Endocr Relat Cancer 2009; 16(3): 663-73.
17. Rosa M, Chopra HK, Sahoo S. Fine needle aspiration biopsy diagnosis of metastatic prostate carcinoma to inguinal lymph node. Diagn Cytopathol 2007; 35(9): 565-7.

經支氣管細針抽吸診斷攝護腺癌併縱膈腔淋巴腺轉移：病例報告

鐘桂彬　何肇基　余忠仁

攝護腺癌可以造成骨轉移或是局部淋巴腺轉移。縱膈腔淋巴腺轉移於攝護腺癌較為罕見，其可以在初診斷時或是治療後發生。在經支氣管鏡超音波尚未發展的年代，縱膈腔淋巴腺轉移需要倚賴侵襲性的術式，例如：縱膈腔鏡、胸腔鏡、或是開胸手術。經支氣管鏡超音波併細針抽吸的應用可以提供縱膈腔淋巴腺腫大良好的診斷資訊。我們在此報告一個67歲的男性攝護腺癌病人，於治療中發生縱膈腔淋巴腺轉移以及肺部癌性淋巴管炎，並由經支氣管鏡超音波併細針抽吸的使用確立診斷。對於攝護腺癌併縱膈腔淋巴腺腫大，攝護腺癌轉移需要納入鑑斷的考慮。其診斷可以利用經支氣管鏡超音波併細針抽吸加以確認，而避免侵襲性較高的診斷術式。*(胸腔醫學* ***2010; 25: 279-285)***

關鍵詞：攝護腺癌，縱膈腔淋巴腺腫大，經支氣管鏡超音波，經支氣管細針抽吸

國立台灣大學醫學院附設醫院　內科部　胸腔內科
索取抽印本請聯絡：何肇基醫師，國立台灣大學醫學院附設醫院　內科部　胸腔內科，100台北市中正區中山南路7號